

# Structural Investigation of Weak Intermolecular Interactions in Fluorine Substituted Isomeric *N*-Benzylideneanilines

Published as part of the *Crystal Growth & Design* virtual special issue In Honor of Prof. G. R. Desiraju

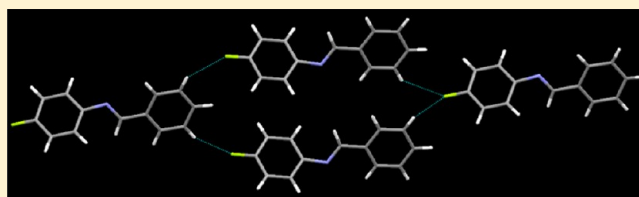
Gurpreet Kaur,<sup>†,‡</sup> Piyush Panini,<sup>‡,‡</sup> Deepak Chopra,<sup>\*,‡</sup> and Angshuman Roy Choudhury<sup>\*,†</sup>

<sup>†</sup>Department of Chemical Sciences, Indian Institute of Science Education and Research (IISER) Mohali, Sector 81, Knowledge City, S. A. S. Nagar, Manauli PO, Mohali, 140306, Punjab, India

<sup>‡</sup>Department of Chemistry, Indian Institute of Science Education and Research Bhopal, Govindpura, Bhopal, 462023, Madhya Pradesh, India

## Supporting Information

**ABSTRACT:** The study of the influence of aromatic C–F group in directing crystal packing is an important area of current research. The role of the aromatic C–F group in the formation of weak intermolecular interactions in the absence of strong hydrogen bond donors and acceptors has been analyzed in a series of 15 newly synthesized fluorine substituted (mono- and di-) isomeric *N*-benzylideneanilines. It was observed that five compounds (out of a total number of 15) were liquids at room temperature, while others have low melting points (<60 °C). *In situ* crystallization, using an optical heating and crystallization device (OHCD), has been used to crystallize and determine the crystal structures of three out of five compounds which were found to be liquids at 25 °C. A detailed investigation of the molecular conformation and the crystal packing in these compounds reveals that the presence of organic fluorine acts as a significant contributor in the construction of various supramolecular synthons, essentially using a variety of C–H...F intermolecular interactions. These have been found to generate different three-dimensional arrangements of molecules in the crystalline framework. In order to realize the stabilizing influence exerted by such weak interactions, intermolecular C–H...F interaction energies have been calculated using Firefly to quantify the strength of such interactions. Lattice energy calculations have been performed and the individual energies, namely, the Coulombic, polarization, dispersion, and repulsive contributions to the lattice energy have been determined using the CLP program. In addition to these, theoretical calculations have been performed at the density functional theory level, and the experimental geometry has been compared with the optimized geometry to highlight the importance of molecular conformation in the solid and gas phase. It is of interest to note that stabilization resulting from the presence of C–H...F interactions, albeit less, is not negligible and does contribute toward crystal packing.



## INTRODUCTION AND AIM OF STUDY

The study of intermolecular noncovalent interactions has been a major theme of contemporary research to study the formation of supramolecular assemblies.<sup>1</sup> Various noncovalent interactions are well recognized in chemistry and biology.<sup>2</sup> Strong hydrogen bonds have been well understood in the literature,<sup>3</sup> and the recent focus is toward understanding the role of weak hydrogen bonds in building supramolecular assemblies of small organic molecules.<sup>4</sup> In recent years, the focus has been extended toward the understanding of intermolecular interactions involving halogens, particularly in the context of organic fluorine.<sup>5a</sup> A C–F group, historically termed as “organic fluorine”,<sup>5b</sup> has been shown to exhibit poor hydrogen bond acceptor properties in the literature.<sup>5c,d</sup> The absence of participation of organic fluorine in intermolecular interactions has been attributed to the nonpolarizable nature of the fluorine atom.<sup>5e</sup> The importance of intermolecular interactions involving organic fluorine has received considerable attention and significant progress has been made in the past decade. A recent review,<sup>6a</sup> a highlight,<sup>6b</sup> and a perspective<sup>6c</sup> have brought out the

importance of organic fluorine in the crystal engineering community. It was realized that, in the absence of strong hydrogen bonds, the molecules containing C–F bond essentially pack utilizing weak C–H...F, C–F... $\pi$ , and C–F...F–C interactions.<sup>7</sup> The focus was then shifted toward analyzing the presence of such weak interactions in the presence of strong H-bonds. In this regard, detailed crystallographic investigations have recently been performed on fluorinated,<sup>8a–c</sup> other halogen substituted,<sup>8d</sup> and also trifluoromethylated<sup>8e</sup> benzanilides containing a strong N–H donor and a strong acceptor such as >C=O group. It was observed that in addition to the well documented N–H...O=C and C–H...O=C hydrogen bonds, the crystal packing was influenced by weak interactions of the type C–H...F–C along with C–F... $\pi$ , C–F...F–C, and C–H... $\pi$  intermolecular contacts in the crystal lattice. In order to evaluate the support provided by weak interactions involving

Received: July 21, 2012

Revised: August 30, 2012

Published: September 4, 2012

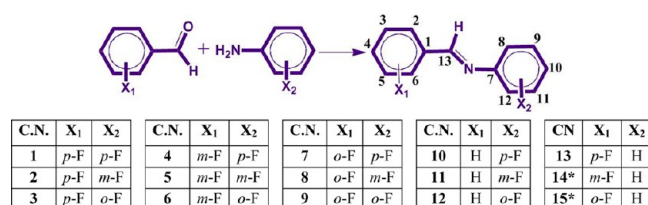
organic fluorine, we have synthesized and crystallized a series of isomeric *N*-benzylideneanilines wherein the amide group has been replaced by an imine functional group, keeping the remaining molecular scaffold invariant when compared to fluorinated benzanilides. This eliminates the possibility of the formation of strong hydrogen bonds and allows one to assess the interplay of other weak interactions in the crystalline solid.

The *N*-benzylideneanilines are an important class of compounds and have important biological properties. A number of patents highlight the versatile application of this class of molecules, for example, in the protection of skin against the harmful effects of sunlight (erythema) on human skin<sup>9a</sup> and warm-blooded animals.<sup>9b</sup> A recent patent highlights the importance of a mixture of *N*-benzylideneaniline compounds with aqueous acid solution being used as corrosion inhibitor.<sup>9c</sup>

In the crystallographic literature, these compounds have a rich history. The initial structural determination was done in 1968.<sup>10a</sup> It was observed that the unsubstituted *N*-benzylideneaniline (parent compound) is nonplanar and the aniline ring is twisted by 57° from the C–N=C–C plane. It was observed that the UV spectra of this compound<sup>10b</sup> was different from that of stilbene<sup>10c</sup> and *trans*-azobenzene<sup>10de</sup> whose crystal structure revealed that those molecules were planar. The crystal structure of *N*-benzylideneaniline was again redetermined using accurate data.<sup>11</sup> In order to account for the nonplanar conformation of this compound, Huckel-Molecular Orbital calculations were performed with an aim to highlight the sensitive nature of energy contributions coming from the  $\pi$ -electron and the nonbonded interactions in this class of molecules.<sup>12</sup> These molecules provide an excellent chemical model to understand the relationship between molecular conformation and electronic/structural features resulting from different substituents present on the molecular framework. The conformational flexibility associated with C–C and C–N bond rotation connected to the two phenyl rings allows different conformers to be trapped/isolated. This leads to the existence of conformational polymorphs. One such example is the case of *N*-(*p*-methylbenzylidene)-*p*-methylaniline which exhibits trimorphic behavior in the solid state (concomitant polymorphism wherein crystals are obtained from ethanol),<sup>13</sup> wherein both planar and nonplanar conformations have been observed in different forms. The energies associated with these conformations have been estimated by *ab initio* calculations. The nonplanar conformation was found to be more stable by 6.57 kJ/mol over the planar conformation.<sup>14</sup> Thus the presence of disorder in the crystalline environment seems to contribute to lattice energy of certain magnitude to stabilize a high energy conformation.<sup>15</sup> Although the Form II had a normal perfectly ordered average structure, three-dimensional (3D) X-ray data collected on this form indicates strong diffuse scattering reflecting the fact that substantial thermal disorder is present.<sup>16</sup> Another case is provided by *p*-chloro-*N*-(*p*-chlorobenzylidene)aniline which exists in the planar triclinic form<sup>17a</sup> and nonplanar monoclinic form.<sup>17b</sup> Lattice energy calculations established the planar form to be stable by 4.39 kJ/mol.<sup>17cd</sup> The conformational flexibility (pedal motion) associated with these compounds results in the existence of different molecular conformations. This has been studied in stilbenes,<sup>18a</sup> azobenzenes,<sup>18b</sup> and cyano substituted benzanilides.<sup>18c</sup> Variable temperature X-ray diffraction data collected on single crystals allow a detailed analysis of both static and dynamic disorder present in the crystals.<sup>18d</sup> This approach has also been applied to investigate conformational changes in nitro, methyl, methoxy, carboxylic, and chloro substituted *N*-benzylideneanilines by Ogawa and co-workers.<sup>18e</sup> The above-mentioned aspects relate well with our

model system containing organic fluorine. It has been documented that the presence of fluorine in the *ortho* or *meta* position of different aromatic molecules generates positional disorder due to their participation in different intermolecular interactions, thus providing stability to the crystal lattice.<sup>7a,19</sup> In the current series, the fluorine atom in the *ortho* and the *meta* positions may also get disordered in order to offer different intermolecular interactions and hence generate different molecular and crystal structures. The purpose is to access the different independent conformations a given molecule can explore (phenomenon of conformational polymorphism) and to understand the nature of disorder (static or dynamic) present in different fluorine substituted compounds. Furthermore, it is of interest to understand the nature and the strength of C–H...F interactions, in fluorine substituted *N*-benzylideneanilines. Fifteen new compounds (Scheme 1) were

**Scheme 1. Chemical Scheme of All the Studied Compounds Where  $X_1 = -H/-F$ ;  $X_2 = -H/-F^a$**



<sup>a</sup>The crystal structures of C.N. 14 and 15 could not be determined.

synthesized and characterized using Fourier transform infrared spectroscopy (FTIR), Nuclear magnetic resonance (NMR), differential scanning calorimetry (DSC), etc. Five of these were found to be liquid at 25 °C. Three of these five liquids could be crystallized using an *in situ*<sup>20</sup> crystallization technique. The crystal structures of 13 compounds have been thoroughly studied for the identification of unique supramolecular motifs involving fluorine in addition to other weak interactions which contribute toward the stability of the crystal packing.

## EXPERIMENTAL SECTION

**Procedure for Synthesis.** All the starting materials, namely, the *ortho*, *meta*, and *para* fluorinated benzaldehydes and the corresponding *ortho*, *meta*, and *para* fluorinated anilines, were purchased from Sigma Aldrich and were used without further purification. Fluorobenzaldehyde (0.02 mol) was added to the solution of fluoroaniline (0.02 mol) in about 25.0 mL of toluene. The reaction mixture was then refluxed for 3 h in the presence of 4 Å activated molecular sieves. The completion of the reaction was monitored by thin layer chromatography (TLC). After completion of the reaction, the mixture was filtered using Whatman filter paper and the resulting solvent was then evaporated. The crude product thus obtained was purified by a neutral column.

**Procedure to Activate Molecular Sieves.** The molecular sieves were first washed with acetone and then kept in the oven at 120 °C for 1 day. These were further activated in the microwave oven for 1.0 min before using them for the reaction.

**Procedure of Neutral Column.** The slurry of 100–200 mesh silica was made in hexane, and then 10–15 mL of triethylamine was added to the same. The column was packed using this slurry. Solution of the crude product in the minimum amount of hexane was loaded into the column. The column was then run by slowly increasing the polarity to 5% ethylacetate/hexane. Distilled hexane and ethylacetate were used for this purpose.

Scheme 1 describes all the molecules studied and the method used for their nomenclature. Out of 15 compounds synthesized, 10 were solids at room temperature while the remaining five compounds [compound numbers (C.N.) 5, 8, 11, 14, and 15] were liquids. One of these (C.N. 9) was found to exhibit polymorphism.

All the synthesized compounds were characterized by FTIR [Figure S1a–o] and  $^1\text{H}$  NMR [Figure S2a–o] spectroscopy. Melting points (Table S1) were recorded and the DSC traces for all the solid compounds are given in the Supporting Information [Figure S3a–j]. Powder X-ray diffraction (PXRD) data were recorded for the solid compounds and compared with the simulated PXRD patterns generated from the crystal coordinates in Mercury 3.0,<sup>21</sup> and the final plots were done in Origin 6.1 [Figure S4a–m]. It has been found that the simulated PXRD patterns were matching with the PXRD patterns recorded on the bulk samples, except for the two polymorphs (polymorphs I and II) of C.N. 9. For compound 9, the experimental profiles for the recorded PXRD pattern were refined with the lattice parameters of both the forms using the program JANA2000.<sup>22</sup> The profile fitting parameters Rp and wRp were 8.77% and 12.89% respectively [Figure S5].

**Crystal Growth, Diffraction Data Collection and Structure Solution.** Single crystals of all the purified solids were grown from different common organic solvents (methanol, ethanol, acetone, chloroform, dichloromethane, hexane, toluene, acetonitrile, etc.) and solvent mixtures (polar and nonpolar solvent combinations) (Table 1) at low temperature (4 °C or –20 °C). All the crystallization products were screened under an optical polarizing microscope for the identification of the crystal morphologies and were then checked by unit cell determination using the single crystal X-ray diffraction (SCXRD) technique for the identification of different polymorphs, if any. Only compound 9 yielded two polymorphs from two different solvents (hexane and methanol). SCXRD data for all the compounds were collected using a Bruker AXS KAPPA APEX-II CCD diffractometer (monochromatic Mo  $K_\alpha$  radiation) equipped with an Oxford cryo-system 700 Plus at 100.0(1) K. Data collection and unit cell refinement for the data sets were done using the Bruker APEX-II<sup>23</sup> suite, data reduction and integration were performed by SAINT V7.685A12 (Bruker AXS, 2009), and the absorption corrections and scaling were done using SADABS V2008/112 (Bruker AXS). The crystal structures were solved by using Olex2<sup>24</sup> or WinGx<sup>25</sup> packages using SHELXS97,<sup>26</sup> and the structures were refined using SHELXL97.<sup>26</sup> All the hydrogen atoms have been geometrically fixed and refined using the riding model. Table 1 lists the crystal and refinement data for 13 compounds. All the packing and the interaction diagrams have been generated using Mercury.<sup>21</sup> Geometric calculations have been done using PARST<sup>27</sup> and PLATON.<sup>28</sup>

**Crystal Growth and Data Collection for Liquids.** Compounds 5, 8, 11, 14, and 15 are liquids at room temperature and were subjected to *in situ* crystallization. In all the cases, the compound was taken in an 0.3 mm Lindemann quartz capillary and was sealed at both ends with glue and was mounted on Bruker AXS KAPPA APEX-II CCD diffractometer with the capillary aligned vertically. For compound 5, the capillary was then cooled at 360 K/h to 200 K but the liquid did not solidify by itself. A zone of the capillary was heated by the CO<sub>2</sub> LASER of the OHCD<sup>29</sup> and suddenly the heat was withdrawn. This was repeated a few times to initiate crystallization in the capillary. Then the capillary was warmed up to 220 K and a few cycles of zone melting scans using the CO<sub>2</sub> LASER of the OHCD were repeated for 3 h to grow a single crystal in the capillary. After the formation of a single crystal, one  $\Phi$  scan (scan width 0.3°, 1200 frames) data were collected keeping  $\omega$  and  $\kappa$  fixed at 0° and the detector fixed at 30° and with a detector distance of 6.0 cm.

For compound 8, the capillary was cooled to 250 K. The liquid solidified to a polycrystalline mass on cooling. Several zone melting scans using the CO<sub>2</sub> LASER were done for about 12–13 h to get single crystals of the compound in the capillary. Similar  $\Phi$  scan data were collected, the scan width being 0.5° (720 frames).

Compound 11, was cooled from 290 to 140 K first at 360 K/h, which resulted in the formation of a glassy material. Then it was warmed to 240 at 200 K/h. Zone melting scans using the CO<sub>2</sub> LASER from bottom to top always resulted in a glassy material. Thereafter, zone melting scans were done from top to bottom for 3 h. This scan resulted in the crystallization of the material, though the crystals were not of very good quality. Similar  $\Phi$  scan data were collected with a scan width 0.3° (1200 frames).

**Crystallographic Modeling of Disorder.** Among all 15 compounds, compounds 1, 4, 5, 7, 9 (both polymorph I and polymorph II), and 11 were found to be disordered. In the case of compounds 1, 5 ( $Z' = 0.5$ ), and both forms of 9, the molecules display positional disorder around the C=N bond which were refined with 0.5 occupancy using the PART command in SHELXL97 and the thermal parameters were constrained to be equal by the EADP command in SHELXL 97 [Figure S6a,e,i]. In the case of the compound 4 ( $Z' = 2$ ), both molecules in the asymmetric unit were found to be disordered at two orientations around the C=N bond with the occupancy ratio of 0.941(2):0.059(2) for molecule A and 0.935(2):0.065(2) for molecule B for 100 K data [Figure S6d]. The corresponding values for 200 K data are 0.946(3):0.054(3) and 0.936(3):0.064(3), and for 298 K data are 0.960(3):0.040(3) and 0.951(3):0.049(3), respectively, indicating the presence of static disorder in the crystal structure. The disorder was analyzed using the PART command in SHELXL97 and refined for two independent positions, namely, A and B (“A” for higher occupancy). For the purpose of refinement, the carbon atom positions for A and B in the benzene ring were fixed at the same position using the EXYZ command in SHELXL97. Thermal parameters were also constrained to be equal for the atoms at the same position using the EADP command in SHELXL97. All hydrogen atoms were then positioned geometrically and refined using a riding model with  $U_{\text{iso}}(\text{H}) = 1.2U_{\text{eq}}(\text{C,N})$ . In the case of the compound 7 (refined with  $Z' = 0.5$ ), the true molecule (possessing fluorine substitution at *para* on aniline side while *ortho* at benzaldehyde side) does not have any symmetry, and the requirement of  $Z' = 0.5$  suggests the presence of crystallographic disorder around the C=N bond, which generates the second half of the molecule around the center of inversion as is depicted in Figure S6g. Careful refinements with equal occupancy at two independent positions (namely, A and B for benzene ring) with similar refinement strategy as mentioned previously for compound 4 were performed. The fluorine atoms in the molecule are also found to be disordered at two independent positions with the occupancy being 0.5 each. The compound 11 (liquid at RT) in the crystal is found to be statistically disordered and carefully refined at two independent orientations, namely, “A” (for major one) and “B” (for minor one), using the PART command in SHELXL97, the final population ratio being 0.850(6):0.150(6) [Figure S6k]. Except fluorine all other atoms in the minor conformer were refined isotropically with thermal parameters of all carbon atoms being constrained to the same value using EADP in SHELXL97. The benzene rings of minor conformer were constrained to be a regular hexagon using FLAT command and C–C bond lengths were restrained to 1.39 Å using DFIX in SHELXL97. The C–C–C bond angles in the benzene ring were also restrained to the same value using the SADI command in SHELXL97. The remaining molecules 2, 3, 6, 8, 10, 12, and 13 do not exhibit any disorder in the crystal structures.

**Theoretical Calculations.** The intermolecular interactions observed in these compounds are of the type C–H $\cdots$ F and C–H $\cdots$  $\pi$  [Table 2]. The sum of the van der Waals radii<sup>30</sup> has been considered as the limiting distance for the evaluation of different interactions present in these compounds. The primary supramolecular motifs which include chains and dimers formed by C–H $\cdots$ F interactions have been used as inputs for the program FIREFLY<sup>31</sup> to calculate interaction energies and the corresponding CIFs were used as input for PIXEL calculations.<sup>32</sup>

The interaction energy (IE) calculations were performed using FIREFLY, previously known as the PC GAMESS, at the density functional theory (DFT) level using B3LYP function and 6-31G as the basis set. GABEDIT<sup>33</sup> was used as a graphical interface for FIREFLY. The primary coordinates for the molecules under study were taken from their respective experimentally determined crystal structures (at 100 K). Table 2a lists all these intermolecular interactions along with their interaction energies. The energies of the different monomers ( $E_{\text{monomer}}$ ) or dimers ( $E_{\text{dimer}}$ ) were calculated at the same level of theory. The stabilization energy of the dimer ( $\Delta E_{\text{dimer}}$ ) was calculated using the formula  $\Delta E_{\text{dimer}} = [E_{\text{dimer}} - (2 \times E_{\text{monomer}})]$ . If the dimer is formed by two identical C–H $\cdots$ F–C interactions, then the corresponding interaction energy is reported as  $\Delta E_{\text{dimer}}/2$ . If the

Table 1. Crystallographic Data for Compounds 1–13

data	1	2	3	4	5	6	7
formula	C <sub>13</sub> H <sub>9</sub> F <sub>2</sub> N						
FW	217.21	217.21	217.21	217.21	217.21	217.21	217.21
CCDC no.	884979	884984	884985	884986	884987	884988	884989
solvent system	EtOH	DCM + hexane	MeOH	DCM	<i>in situ</i>	ACN	MeOH
morphology	plate	block	needle	plate	<i>in situ</i>	block	block
crystal system	triclinic	monoclinic	monoclinic	triclinic	monoclinic	orthorhombic	monoclinic
space group	$P\bar{1}$	$P2_1/c$	$P2_1$	$P\bar{1}$	$P2_1/c$	$P2_12_12_1$	$P2_1/c$
<i>a</i> (Å)	5.728(5)	14.530(3)	6.0664(3)	7.252(5)	7.212(2)	6.4645(2)	7.202(2)
<i>b</i> (Å)	7.416(5)	5.747(1)	14.1400(5)	11.594(5)	5.862(1)	12.0553(4)	5.900(1)
<i>c</i> (Å)	12.487(5)	12.345(3)	12.0036(5)	13.535(5)	12.443(3)	13.1914(4)	12.292(2)
$\alpha$ (°)	105.745(5)	90	90	64.666(5)	90	90	90
$\beta$ (°)	98.559(5)	107.326(1)	90.228(2)	75.500(5)	108.521(2)	90	108.789(6)
$\gamma$ (°)	90.003(5)	90	90	89.803(5)	90	90	90
volume (Å <sup>3</sup> )	504.4(6)	984.1(4)	1029.65(8)	988.8(9)	498.9(2)	1028.03(6)	494.4(1)
Z	2	4	4	4	2	4	2
$\rho$ (g/cm <sup>3</sup> )	1.43	1.466	1.401	1.459	1.446	1.403	1.459
$\mu$ (mm <sup>-1</sup> )	0.110	0.113	0.108	0.112	0.111	0.108	0.112
F(000)	224	448	448	448	224	448	224
$\theta_{\min,\max}$	1.72, 25.03	2.94, 25.02	1.70, 25.03	1.73, 25.03	2.98, 24.98	2.29, 24.99	2.99, 25.02
$h_{\min,\max}; k_{\min,\max}; l_{\min,\max}$	-6, 5; -8, 8; -14, 14;	-16, 17; -3, 6; -14, 14	-3, 7; -16, 16; -14, 13	-8, 8; -13, 13; -16, 15	-8, 8; -3, 3; -14, 14	-6, 7; -14, 14; 15, 15	-8, 8; -5, 7; -14, 13
no. of reflections.	7796	5454	5976	11528	2208	19712	3719
no. unique/observed reflections.	1761/1513	1734/1639	3448/3327	3474/3181	606/579	1815/1766	864/752
no. of parameters	145	145	290	303	74	145	79
wR <sub>2</sub> _obs, R_obs	0.117, 0.045	0.0996, 0.0331	0.0655, 0.026	0.1618, 0.0582	0.0752, 0.0273	0.1117, 0.0367	0.1466, 0.0454
$\Delta\rho_{\min,\max}$ (e Å <sup>-3</sup> )	-0.277, 0.429	-0.198, 0.259	-0.134, 0.124	-0.443, 0.787	-0.193, 0.104	-0.181, 0.410	-0.305, 0.356
GOF	1.126	1.039	1.078	1.092	1.082	1.132	1.172
data	8	9F1	9F2	10	11	12	13
formula	C <sub>13</sub> H <sub>9</sub> F <sub>2</sub> N	C <sub>13</sub> H <sub>9</sub> F <sub>2</sub> N	C <sub>13</sub> H <sub>9</sub> F <sub>2</sub> N	C <sub>13</sub> H <sub>10</sub> FN			
FW	217.21	217.21	217.21	199.22	199.22	199.22	199.22
CCDC no.	884990	884991	884992	884980	884981	884982	884983
solvent system	<i>in situ</i>	hexane	MeOH	EtOH	<i>in situ</i>	DCM + hexane	DCM + hexane
morphology	<i>in situ</i>	plate	plate	plate	<i>in situ</i>	thin rod	block
crystal system	monoclinic	monoclinic	orthorhombic	monoclinic	monoclinic	orthorhombic	triclinic
space group	$P2_1/c$	$P2_1/c$	$P2_12_12_1$	$P2_1/n$	$P2_1/c$	$P2_12_12_1$	$P\bar{1}$
<i>a</i> (Å)	15.393(9)	9.8109(9)	3.8396(6)	5.6613(1)	12.022(2)	6.3184(3)	5.594(1)
<i>b</i> (Å)	3.851(2)	3.7789(3)	11.871(2)	25.0212(5)	7.913(2)	12.0035(6)	7.225(1)
<i>c</i> (Å)	22.616(2)	27.044(3)	22.205(4)	7.1416(1)	12.242(4)	13.3787(7)	12.569(2)
$\alpha$ (°)	90	90	90	90	90	90	91.99(1)
$\beta$ (°)	132.377(7)	90.991(5)	90	90.216(1)	119.589(2)	90	97.70(1)
$\gamma$ (°)	90	90	90	90	90	90	90.29(1)
volume (Å <sup>3</sup> )	990.3(10)	1002.5(2)	1012.2(3)	1011.62(3)	1012.8(4)	1014.68(9)	503.1(2)
Z	4	4	4	4	4	4	2
$\rho$ (g/cm <sup>3</sup> )	1.457	1.439	1.425	1.308	1.307	1.304	1.315
$\mu$ (mm <sup>-1</sup> )	0.112	0.111	0.110	0.090	0.090	0.089	0.090
F(000)	448	448	448	416	416	416	208
$\theta_{\min,\max}$	2.44, 25.02	1.51, 25.01	1.95, 27.48	1.63, 23.53	3.21, 25.02	2.28, 25.02	2.82, 26.35
$h_{\min,\max}; k_{\min,\max}; l_{\min,\max}$	-18, 18; -2, 2; -26, 26	-11, 11; -4, 4; -32, 31	-4, 4; -10, 15; -23, 28	-6, 6; -27, 27; -8, 7	-14, 14; -6, 6; -14, 14	-7, 7; -13, 14; -15, 7	-6, 6; -9, 9; -15, 15
no. of reflections.	4157	8802	8465	6169	4446	2946	6030
no. unique/observed reflections.	1266/1062	1781/1555	2299/2144	1494/1356	1395/1290	1724/1612	2034/1635
no. of parameters	145	145	145	136	185	136	136
wR <sub>2</sub> _obs, R_obs	0.2054, 0.076	0.093, 0.0342	0.0916, 0.0335	0.0796, 0.0315	0.2592, 0.1032	0.0940, 0.0368	0.1051, 0.0414
$\Delta\rho_{\min,\max}$ (e Å <sup>-3</sup> )	-0.584, 0.360	-0.193, 0.390	-0.278, 0.226	-0.181, 0.305	-0.349, 0.760	-0.17, 0.327	-0.202, 0.450
GOF	1.109	1.102	1.125	1.048	1.168	1.061	1.046

dimer is formed by two different C–H...F–C interactions, then the combined interaction energy is reported. If only one such interaction is present between the two interacting molecules then the interaction

energy is taken as  $\Delta E_{\text{dimer}}$ . Lattice energies of these molecules were calculated using the CLP package. The results from the CLP package indicated contributions of Coulombic, dispersion, polarization, and

Table 2. (a) Intermolecular C–H...F and C–H...N Interactions in All the Crystallized Compounds<sup>a</sup> and (b) Intermolecular C–H... $\pi$  and C–F... $\pi$  Interactions<sup>b</sup>

(a) Intermolecular C–H...F and C–H...N Interactions						
CN	C–H...F	symmetry code	C...F (Å)	H...F (Å)	$\angle$ C–H...F (deg)	IE (kcal/mol)
1	C5–H5...F1	$x, y + 1, z + 1$	3.361(2)	2.57	130	–2.46
	C11–H11...F2	$x - 1, y - 1, z - 1$	3.372(2)	2.58	129	–2.33
2	C5–H5...F2	$-x + 1, -y, -z + 1$	3.219(1)	2.48	125	–1.40
	C12–H12...F1 <sup>c</sup>	$x, -y - 1/2, z - 1/2$	3.469(1)	2.44	159	–1.73
	C10–H10...F1	$-x, 1 - y, -z$	3.326(2)	2.56	137	–1.53
3	C13–H13...F1	$x + 1, y, z$	3.214(7)	2.18	160	–4.93
	C9–H9...F2	$x, y, z - 1$	3.357(8)	2.58	128	–0.95
	C26–H26...F3	$x - 1, y, z$	3.242(7)	2.20	161	–4.74
4	C22A–H22A...F3A	$-x, -y + 1, -z - 1$	3.354(4)	2.47	138	–1.70
	C4A–H4A...F2A	$-x + 1, -y, -z + 2$	3.318(3)	2.47	134	–1.61
	C17A–H17A...F4A	$-x, -y, -z + 1$	3.274(4)	2.45	133	–1.57
	C4A–H4A...F1A	$x, +y, +z + 1$	3.366(1)	2.62	125	–2.00
	C12A–H12A...F4A <sup>c</sup>	$-x, -y, -z + 1$	3.494(3)	2.47	159	–2.25
	C15A–H15A...F2A <sup>c</sup>	$x, y, z - 1$	3.513(4)	2.50	155	–1.85
5	C4–H4...F1	$-x + 2, -y, -z + 1$	3.322(1)	2.49	133	–1.62
	C6–H6...F1 <sup>c</sup>	$x, -y - 1/2, z - 1/2$	3.483(2)	2.48	154	–2.59
6	C13–H13...F1	$x - 1, y, z$	3.392(3)	2.35	162	–4.92
7	C5A–H5A...F2	$-x + 2, -y, -z + 1$	3.277(3)	2.44	133	–0.50
	C7–H7...F1	$-x + 1, -y + 1, -z$	3.15(3)	2.22	144	–1.00
	C5A–H5A...F1 <sup>c</sup>	$x, -y + 1/2, z + 1/2$	3.241(4)	2.44	125	–1.79
8	C8–H8...F1	$-x + 1, y - 1/2, -z + 1/2$	3.470(7)	2.41	168	–5.65
	C13–H13...F1	$-x + 1, y - 1/2, -z + 1/2$	3.546(6)	2.53	156	
9F1	C5–H5...F1	$-x, -y + 1, -z + 1$	3.377(2)	2.59	129	–3.48
9F2	C4–H4...F1	$-x + 1, y + 1/2, -z + 1/2$	3.335(2)	2.54	130	–4.39
	C11–H11...F1	$x - 1/2, -y + 1/2, -z$	3.588(2)	2.51	176	–2.34
10	C3–H3...F1	$-x - 1/2, y + 1/2, -z + 1/2$	3.255(2)	2.58	120	–1.38
	C5–H5...F1	$-x + 3/2, y + 1/2, -z + 1/2$	3.354(2)	2.61	126	–1.64
11	C8A–H8A...F1A	$x, -y + 1/2, z + 1/2$	3.41(1)	2.37	161	–3.25
12	C13–H13...F1	$x - 1, y, z$	3.387(2)	2.32	168	–3.87
	C8–H8...N1	$x - 1/2, -y + 3/2, -z + 2$	3.552(2)	2.61	145	–0.42
13	C9–H9...F1	$x, y, 1 + z$	3.290(2)	2.61	120	–1.27
	C11–H11...F1	$-1 + x, y, 1 + z$	3.272(2)	2.56	122	–1.33
	C6–H6...N1	$-x + 2, -y + 1, -z$	3.510(2)	2.67	135	–1.29
(b) Intermolecular C–H... $\pi$ and C–F... $\pi$ Interactions						
CN	C–H/F... $\pi$	symmetry code	C... $\pi$ (Å)	H/F... $\pi$ (Å)	$\angle$ C–H/F... $\pi$ (deg)	
1	C2–H2...Cg2	$1 - x, 2 - y, -z$	3.506 (2)	2.86	126	
	C5–H5...Cg2	$2 - x, 1 - y, -z$	3.526(2)	2.82	131	
	C8–H8...Cg1	$1 - x, 1 - y, -z$	3.461(2)	2.77	130	
	C11–H11...Cg1	$2 - x, 2 - y, -z$	3.544 (2)	2.85	130	
2	C3–H3...Cg1	$1 - x, 1/2 + y, 3/2 - z$	3.460(1)	2.80	129	
	C6–H6...Cg2	$x, 1/2 - y, 1/2 + z$	3.448(1)	2.81	125	
	C8–H8...Cg1	$x, 3/2 - y, -1/2 + z$	3.469(1)	2.74	134	
	C11–H11...Cg2	$-x, -1/2 + y, 1/2 - z$	3.441(1)	2.73	133	
3	C16–H16...Cg2	$x, y, z$	3.448(6)	2.80	126	
	C8–H8...Cg4	$-x, y + 1/2 - z + 1$	3.444(7)	2.66	140	
	C21–H21...Cg2	$-x + 1, y - 1/2, -z + 1$	3.414(6)	2.63	140	
	C11–H11...Cg3	$x + 1, y, z$	3.642(7)	2.87	139	
	C25–F3...Cg1	$x - 1, y, z + 1$	4.006(6)	3.117(5)	122(1)	
4	C3A–H3A...Cg4	$x + 1, y, z + 1$	3.478(4)	2.80	129	
	C16A–H16A...Cg1	$-x + 1, -y, -z + 1$	3.460(4)	2.80	127	
	C6A–H6A...Cg3	$-x, -y, -z + 1$	3.522(4)	2.84	130	
	C19A–H19A...Cg2	$x - 1, y, z$	3.491(4)	2.85	126	
	C8A–H8A...Cg4	$-x + 1, -y + 1, -z$	3.463(4)	2.78	130	
	C21A–H21A...Cg1	$x, y, z - 1$	3.465(4)	2.75	132	
	C11A–H11A...Cg3	$x, y, z$	3.436(4)	2.75	130	
5	C24A–H24A...Cg2	$-x, 1 - y, -z$	3.439(4)	2.72	133	
	C2–H2...Cg1	$1 - x, 1/2 + y, 1/2 - z$	3.512(2)	2.84	129	
	C5–H5...Cg1	$-x, -1/2 + y, 1/2 - z$	3.443(2)	2.75	130	

Table 2. continued

(b) Intermolecular C–H... $\pi$ and C–F... $\pi$ Interactions						
6	C4–H4...Cg2	$1 - x, 1/2 + y, 1/2 - z$	3.625(6)	2.78	149	
	C10–H10...C13 <sup>d</sup>	$3/2 - x, -y, 1/2 + z$	3.736(1)	2.89	149	
7	C3A–H3A...Cg1	$1/2 + x, 1 - y, -1/2 + z$	3.535(4)	2.86	131	
	C6A–H6A...Cg1	$-1/2 + x, -y, -1/2 + z$	3.451(3)	2.78	130	
10	C2–H2...Cg2	$1/2 + x, 1/2 - y, -1/2 + z$	3.407(2)	2.72	131	
	C9–H9...Cg1	$1/2 + x, 1/2 - y, 1/2 + z$	3.552(2)	2.84	134	
	C11–H11...Cg1	$-1/2 + x, 1/2 - y, -1/2 + z$	3.514(2)	2.84	130	
11	C5A–H5A...Cg2	$1 - x, -y, -z$	3.605(9)	2.86	136	
12	C4–H4...Cg2	$2 - x, -1/2 + y, 1/2 - z$	3.617(2)	2.78	148	
	C10–H10...C13 <sup>d</sup>	$3/2 - x, 1 - y, 1/2 + z$	3.717(1)	2.86	150	
13	C3–H3...Cg2	$1 - x, -y, -z$	3.506(2)	2.82	129	
	C5–H5...Cg2	$2 - x, 1 - y, -z$	3.538(2)	2.83	132	
	C8–H8...Cg1	$1 - x, 1 - y, -z$	3.478(2)	2.71	136	
	C12–H12...Cg1	$2 - x, -y, -z$	3.610(2)	2.92	128	

<sup>a</sup>The values in italics indicate “neutron-corrected” distances. The C–H bond distances for X-ray and neutron data are 0.95 Å and 1.08 Å, respectively. <sup>b</sup>Cg1, Cg2, Cg3, and Cg4 refer to the center of gravity of the ring formed by C1–C6, C7–C12, C14–C19, and C20–C25 respectively. <sup>c</sup>These have contributions both from C–H... $\pi$  and C–H...F interactions. <sup>d</sup>Refers to the imine double bond.

repulsive components to the total lattice energy [Table S2]. DFT calculations using B3LYP/6-31G basis set were performed using FIREFLY with crystallographic coordinates as a starting set (only the major conformers were introduced in the calculations in the case of disordered molecules) to obtain the optimized geometry of an isolated molecule. Selected torsion angles obtained from theoretical calculations were compared with the experimentally obtained values (Table 3).

## RESULTS

Figures S6a–m show the ORTEP for all the compounds. All the dihedral angles between the least-squares planes containing the aniline and benzaldehyde moiety are contained in Table S3.

It is of interest to note that the presence of electron withdrawing fluorine atoms is responsible for increasing the acidity of the neighboring hydrogen atoms in the phenyl ring, in addition to the imine hydrogen which is highly acidic and participates in the interactions as well (Table 2). In the absence of strong hydrogen bond donors, the salient features associated with the crystal packing of all the compounds in the current study essentially consist of C–H...F and C–H... $\pi$  intermolecular interactions.

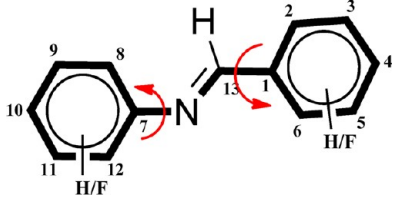
**1. 4-Fluoro-N-(4-fluorobenzylidene)aniline.** Compound **1** crystallizes in the centrosymmetric triclinic  $P\bar{1}$  space group with  $Z = 2$  [Figure S6a]. The central C=N bond exhibits positional disorder, the two independent conformations being present in a 1:1 ratio. The C–H...F interactions, involving H5 with F1 (IE = –2.46 kcal/mol) and H11 with F2 (IE = –2.33 kcal/mol) respectively, pack the molecules to generate molecular sheets [Figure 1a, Table 2a]. These sheets are further interconnected *via* weak C–H... $\pi$  intermolecular interactions forming dimers in the solid state [Figure 1b] (Table 2b).

**2. 3-Fluoro-N-(4-fluorobenzylidene)aniline.** Compound **2** was found to crystallize in the monoclinic centrosymmetric  $P2_1/c$  space group [Figure S6b]. Molecules related to each other by the inversion center were found to form molecular layers by head to head and tail to tail dimers, involving acidic hydrogens H10 and H5 with F1 and F2 respectively [Figure 2, Table 2a]. The molecular layers were again found to interact through weak C–H...F interactions, involving H12 and F1, propagating along the  $c$ -glide along with C–H... $\pi$  interactions (involving H3, H6, H8, and H11) (Table 2). The interactions energies associated with these C–H...F interactions were found to lie between –1.4 to –1.8 kcal/mol (Table 2a), which

indicate weak but significant contribution toward stabilization of crystal structure by these interactions.

**3. 2-Fluoro-N-(4-fluorobenzylidene)aniline.** Compound **3** crystallizes in the monoclinic noncentrosymmetric  $P2_1$  space group with two molecules (A and B) in the asymmetric unit connected *via* a weak C–H... $\pi$  hydrogen bond [Figure S6c] (Table 2b). Both the molecules (A and B) present in the asymmetric unit are found to form molecular chains through short, highly directional, and significantly stabilizing C–H...F interactions involving the highly acidic imine hydrogen H13 with F1 [2.18 Å, 160°, –4.93 kcal/mol] and H26 with F3 [2.20 Å, 161°, –4.74 kcal/mol] respectively [Figure 3a, Table 2a]. The molecular chains are interlinked by the utilization of weak C–H... $\pi$  (involving H8, H11 and H21) and C–F... $\pi$  (involving F3 with Cg1) interactions, and thus alternating ...ABAB... layers along the crystallographic  $b$ -axis are generated [Figure 3b].

**4. 4-Fluoro-N-(3-fluorobenzylidene)aniline.** Compound **4** crystallizes in the triclinic centrosymmetric  $P\bar{1}$  space group with two molecules (A and B) in the asymmetric unit connected *via* a weak C–H... $\pi$  interaction [Figure S6d]. Both molecules in the asymmetric unit were found to be disordered at two orientations around the C=N bond, and this was modeled carefully as described earlier in the Experimental Section, the ratio of the major and minor conformer being 0.941(2):0.059(2) for molecule A and 0.935(2):0.065(2) for molecule B for 100 K data. The population of the two conformers remained invariant when the crystal data were collected at 200 K and 298 K respectively, indicating the presence of static disorder. The atoms in the major conformer of both the molecules were considered for intermolecular interactions analysis (Table 2). The packing of molecule A parallel to the  $bc$  plane displays the formation of a layer motif with the utilization of weak C–H...F interactions (involving acidic hydrogens H4A with F2A and H4A with F1A forming dimeric motifs) [Figure 4a]. Another dimeric pair of C–H...F interactions, involving acidic hydrogens H22A with F3A and H17A with F4A pack the molecules B to generate layers parallel to the  $bc$  plane [Figure 4a]. These two layers of molecules A and B are interconnected by weak C–H... $\pi$  and C–H...F (involving H12A with F4A and H15A with F2A) intermolecular interactions [Figure 4a,b] (Table 2) in the crystal lattice. The interaction energies evaluated for all C–H...F interactions present in the crystal packing range between 1.50 and 2.5 kcal/mol.

Table 3. Selected Torsion Angles ( $^{\circ}$ )<sup>a</sup>


torsion angle	C8–C7–N1–C13–C21–C20–N2–C26 <sup>b</sup>	C6–C1–C13–N1–C19–C14–C26–N2 <sup>b</sup>	C1–C13–N1–C7–C14–C26–N2–C20 <sup>b</sup>
N-benzylideneaniline	56.83(2) 34.94	9.92(2) 0.88	179.51(2) 176.92
compound 1	44 (2), 36.7(16) <sup>c</sup>	6.7(19), 18(2) <sup>c</sup>	177.1(11), 180.0(13) <sup>c</sup>
compound 2	35.59 14.73(16)	1.70 11.76(16)	178.31 178.87(8)
compound 3	34.08 42.6(8), 44.9(8) <sup>b</sup>	1.09 10.7(9), 9.0(9) <sup>b</sup>	176.88 175.6(5), 177.2(5) <sup>b</sup>
compound 4	41.78, 42.72 4.7(4), 14.7(4) <sup>b</sup>	8.44, 7.62 4.6(4), 12.8(4) <sup>b</sup>	173.97, 175.55 179.6(2), 178.1(2) <sup>b</sup>
compound 5 (half molecule)	27.20, 36.16 8.22(5)	1.97, 2.47 10.26(7)	176.75, 176.97 178.92(6)
compound 6	33.09 35.0(3)	0.59 0.6(3)	177.07 178.25(16)
compound 7	38.43 12(3)	0.02 19(3)	176.12 172(2)
compound 8	31.1 39.7(8)	0.70 5.8(9)	177.07 174.1(5)
compound 9 form I	32.27 42.2(12), 43.3(12) <sup>c</sup> , 36.98	0.64 5.5(13), 4.8(14) <sup>c</sup> , 0.75,	177.14 175.6(2), 177.5(3) <sup>c</sup> , 176.23,
compound 9 form II	20.3(7), 25.3(4) <sup>c</sup> 37.41	2.0(5), 29.0(8) <sup>c</sup> , 0.45	176.09 163.0(8), 168.6(8) <sup>c</sup> , 176.09
compound 10	46.5 (2) 33.28	7.7(2) 0.82	178.8(1) 176.95
compound 11	50.4(10) 36.77	8.2(11) 1.08	175.6(8) 176.68
compound 12	33.5(3) 39.18	2.6(3) 0.28	178.64(15) 176.03
compound 13	38.8(2) 34.48	17.7(2) 1.12	179.26(12) 176.88

<sup>a</sup>Only major conformers were considered for disordered molecules. Values in *italics* are obtained from theoretical B3LYP/6-31G calculations. <sup>b</sup>Equivalent torsion angle for the second molecule in the asymmetric unit. <sup>c</sup>Another torsion angle due to the presence of disorder around the C=N bond.

**5. 3-Fluoro-N-(3-fluorobenzylidene)aniline.** The compound was found to crystallize in the monoclinic centrosymmetric space group  $P2_1/c$  with  $Z = 2$  ( $Z' = 0.5$ ). The  $Z' = 0.5$  in the true molecule (possessing fluorine substitution at *meta* position on both sides of the ring) having no symmetry suggests the presence of static disorder around the imine bond (C=N) which generates the second half of the molecule around the center of inversion [Figure S6e]. In the crystal lattice, the molecules are found to pack through linear chains involving dimeric C–H...F intermolecular interactions, namely, H4 with F1 (–1.62 kcal/mol) [Figure 5] (Table 2a), which connect with the other chains in the lattice by another independent set of C–H...F interactions, involving H6 with F1 (–2.59 kcal/mol)

and C–H... $\pi$  interactions, involving H2 and H5 of the aromatic ring [Figure 5] (Table 2).

**6. 2-Fluoro-N-(3-fluorobenzylidene)aniline.** Compound 6 was found to crystallize in the orthorhombic noncentrosymmetric  $P2_12_12_1$  space group with  $Z = 4$  [Figure S6f]. A short and highly directional C–H...F interaction, involving the sufficiently acidic imine hydrogen H13 and F1 [2.35 Å, 162°] forms a molecular ladder along the crystallographic  $a$  axis [Figure 6a, Table 2b]. The interaction energy associated with the C–H...F hydrogen bond is found to be one of the most stabilizing (–4.92 kcal/mol), among all 13 crystal structures. The weak C–H... $\pi$  (involving H4 and H10 with imine carbon utilizes the  $2_1$  screw parallel to  $b$ -axis) intermolecular interactions linked such chains [Figure 6a, Table 2b]. The packing of the molecules was found to display the herringbone pattern when viewed down the crystallographic  $bc$  plane in the crystal structure [Figure 6b].

**7. 4-Fluoro-N-(2-fluorobenzylidene)aniline.** Compound 7 crystallizes in the monoclinic space group  $P2_1/c$  with  $Z = 2$  ( $Z' = 0.5$ ) [Figure S6g]. The disorder associated with this molecule was carefully refined (as is mentioned in the Experimental Section). The crystal packing of the molecules involves the generation of a molecular sheet down the  $bc$  plane [Figure 7a] (Table 2a) *via* dimeric C–H...F intermolecular interactions, involving acidic hydrogens H5A with F2 (–0.50 kcal/mol) and H7 with F1 (–1.00 kcal/mol). Furthermore, the C–H... $\pi$  interactions, involving H6A and H3A, along with C–H...F intermolecular interactions, involving H5A and F1 (–1.79 kcal/mol), provide additional stability to the crystal packing in between the sheet-like structure [Figure 7b] (Table 2b).

**8. 3-Fluoro-N-(2-fluorobenzylidene)aniline.** Compound 8 was indexed to a monoclinic space group  $P2_1/c$  with  $Z = 4$  [Figure S6h]. The molecules were found to form heterodimers by C–H...F interactions, involving H8 and H13 with F1 (the total interaction energy is –5.65 kcal/mol) [Figure 8a, Table 2a], which extend over the crystal lattice [Figure 8b]. The molecular dimer is further connected with another dimer, propagating along the crystallographic  $b$ -axis *via* C–H...F (again involving H8 and H13 with F1) interactions and thus generating a chain of heterodimers along that axis.

**9A. 2-Fluoro-N-(2-fluorobenzylidene)aniline (Polymorph I).** Compound 9 was found to have two polymorphs I and II, but with similar plate-like morphology. Polymorph I was crystallized from the nonpolar solvent hexane, while polymorph II was crystallized from the polar solvent methanol (MeOH). In both polymorphs, the conformational disorder exists around the C=N bond, the ratio of both conformers being 1:1. Polymorph I was solved in monoclinic  $P2_1/c$  space group with  $Z = 4$  [Figure S6(i)-1]. Discrete molecular dimers have been found to form by weak C–H...F intermolecular interactions (involving H5 with F1, –3.48 kcal/mol) in the crystal packing, and no other significant interactions were observed between these dimers forming molecular sheets in the solid [Figure 9a] (Table 2a).

**9B. 2-Fluoro-N-(2-fluorobenzylidene)aniline (Polymorph II).** The polymorph II of 9 was found to crystallize in the orthorhombic noncentrosymmetric  $P2_12_12_1$  space group with  $Z = 4$  [Figure S6(i)-2]. The molecules in the crystal pack *via* the formation of zigzag chains, utilizing weak C–H...F intermolecular interactions, involving H4 with F1 (utilize  $2_1$  screw, –4.39 kcal/mol) along the crystallographic  $b$ -axis [Figure 9b, Table 2a]. Another C–H...F intermolecular interaction

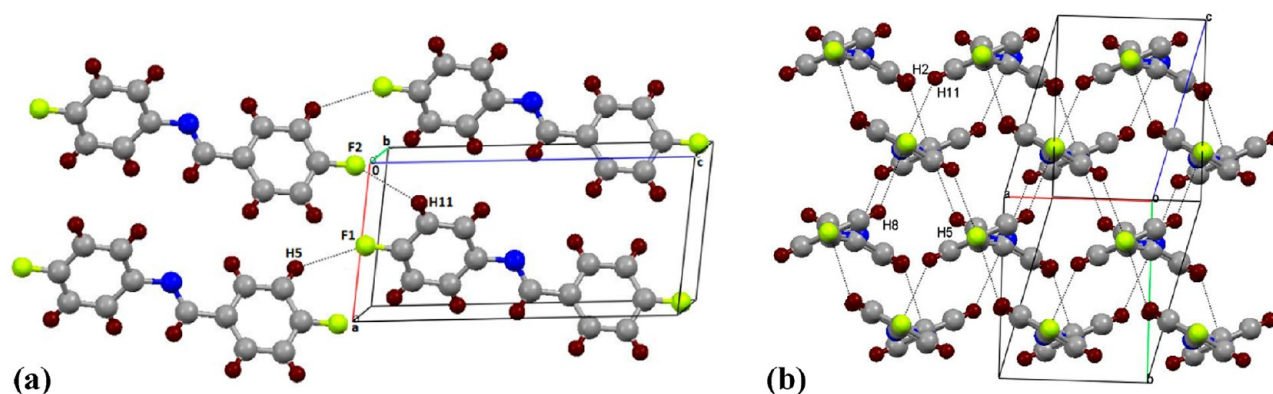


**Figure 1.** (a) Formation of sheets viewed down the  $ac$  plane by  $C-H\cdots F$  interactions in **1**. Disordered atoms were omitted for clarity. (b) Formation of a molecular layer *via* weak  $C-H\cdots\pi$  interactions in **1**.

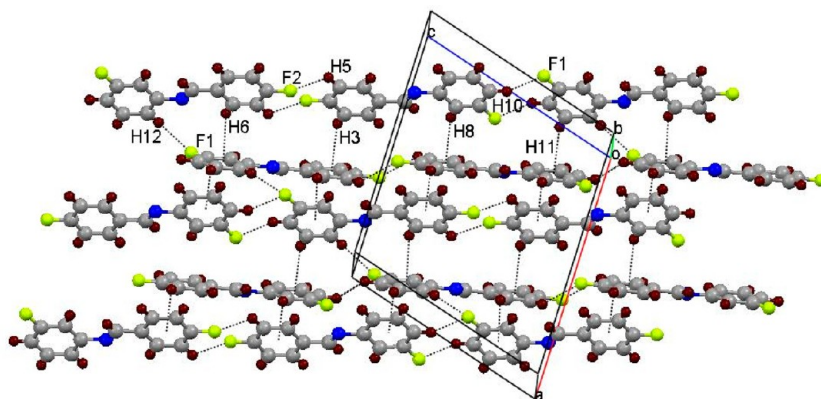


**Figure 2.** Formation of molecular layers by  $C-H\cdots F$  and  $C-H\cdots\pi$  intermolecular interactions in **2**.

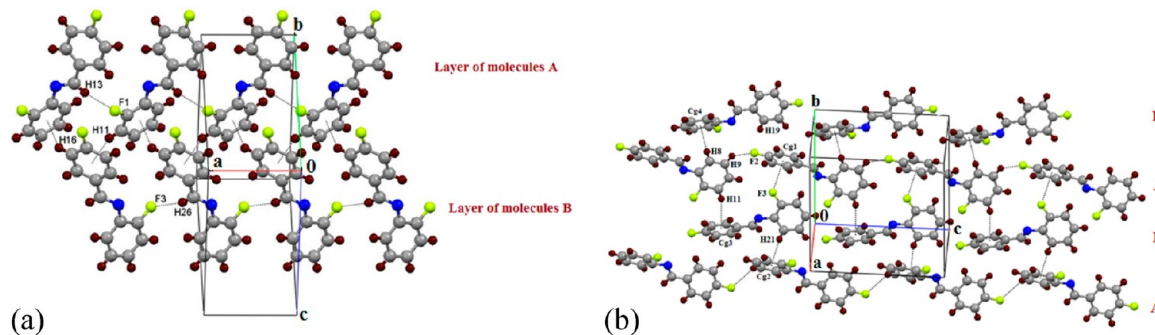


**Figure 3.** (a) Packing view displaying formation of molecular chains of both molecules of the asymmetric unit along the crystallographic  $a$ -axis which are connected through  $C-H\cdots\pi$  interactions in **3**. (b) Formation of alternate ...ABAB... layers *via* the network of weak  $C-H\cdots\pi$ ,  $C-H\cdots F$ , and  $C-F\cdots\pi$  interactions in **3**.

involving H11 with F1 ( $-2.34$  kcal/mol) with the utilization of  $2_1$  connects the above-mentioned chain down the crystallographic  $a$ -axis [Figure 9b, Table 2a]. It is of interest to note that there are no  $C-H\cdots\pi$  intermolecular interactions present in both the crystal forms of **9**.

**10. *N*-Benzylidene-4-fluoroaniline.** This compound crystallizes in the monoclinic centrosymmetric  $P2_1/n$  space group [Figure S6j]. Packing in the crystal involves the formation of molecular sheet motif with the utilization of bifurcated weak  $C-H\cdots F$  intermolecular interactions, involving H3 and H5 with F1 ( $-1.38$  kcal/mol and  $-1.64$  kcal/mol respectively) propagating along the  $2_1$  screw down the crystallographic  $b$ -axis [Figure 10a, Table 2]. Weak  $C-H\cdots\pi$  (involving H2 with Cg2, H9 and H11 with Cg1) intermolecular interactions stabilize the

layer motif, with the utilization of the  $n$  glide plane of symmetry [Figure 10b, Table 2b].

**11. *N*-Benzylidene-3-fluoroaniline.** Compound **11** crystallizes in the monoclinic centrosymmetric  $P2_1/c$  space group with  $Z = 4$  [Figure S6k]. It is of interest to note that *in situ* crystallization of the low-melting liquid results in trapping of both the major and minor conformer of this molecule. It is to be noted that a  $180^\circ$  rotation of the entire molecule around the shorter axis results in the occurrence of the observed conformations. This kind of a molecular rotational process is very rare as it involves steric interactions with the neighboring molecules in the crystalline lattice.<sup>18d</sup> This feature of molecular disorder has also been observed in *N*-benzylideneaniline and *N*-(4-methoxybenzylidene)-4-methylaniline.<sup>18d</sup>

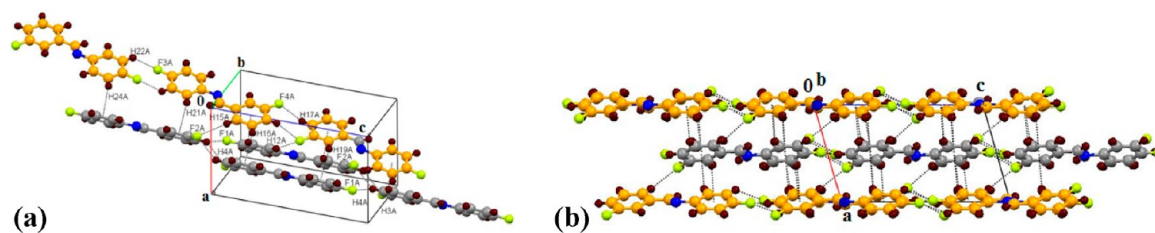


**Figure 4.** (a) Formation of layered motifs by both molecules (shown with different colors: gray and orange) of asymmetric unit *via* weak C–H...F and C–H... $\pi$  interactions in **4**. The disordered hydrogen and carbon atoms having a lower occupancy have been omitted for clarity. (b) Packing viewed down the *ac* crystallographic plane, displaying the formation of alternate layers of molecular sheets of A (gray) and B (orange) *via* C–H...F and C–H... $\pi$  interactions in **4**.

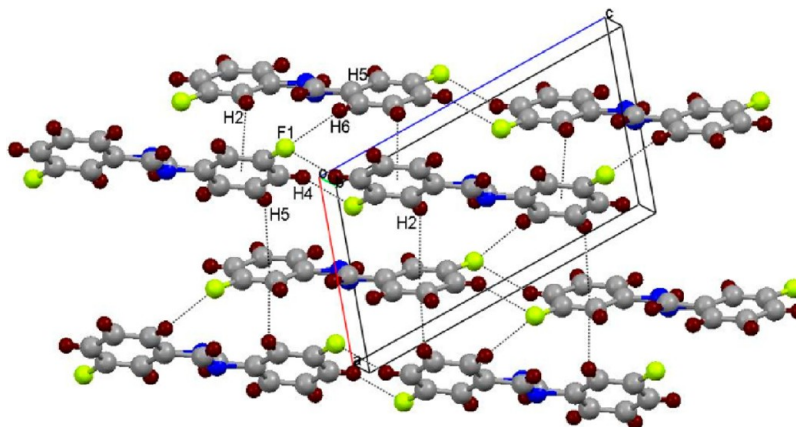


**Figure 5.** Packing of the molecules of **5** viewed down the *ac* plane displaying formation of layers through C–H...F and C–H... $\pi$  intermolecular interactions.

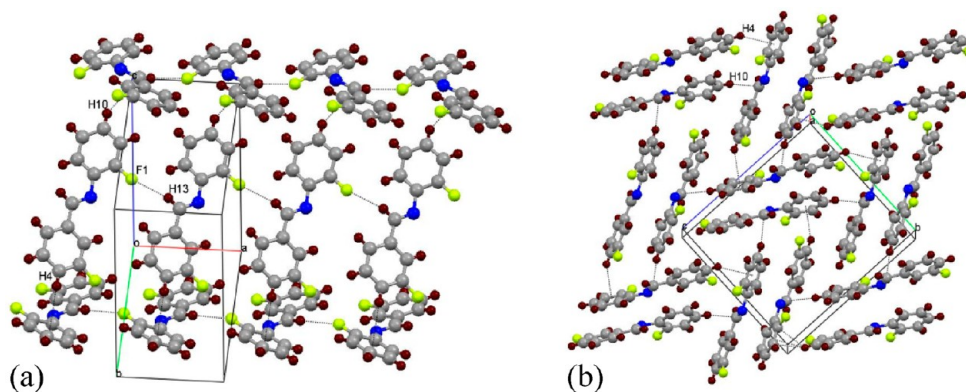


**Figure 6.** (a) Formation of a molecular ladder down the *ac* plane by C–H...F intermolecular interactions in **6**. (b) Packing viewed down the *bc* plane, showing the formation of herringbone motifs by the utilization of C–H... $\pi$  interactions in **6**.

In **11**, the packing of molecules involves the formation of molecular chains, *via* weak C–H...F interactions (involving H8A with F1A,  $-3.25$  kcal/mol) with the utilization of *c*-glide plane [Figure 11, Table 2a]. The chains are further linked with dimeric C–H... $\pi$  intermolecular interactions (involving H5A) [Figure 11, Table 2b].

**12. N-Benzylidene-2-fluoroaniline.** Compound **12** crystallizes in the orthorhombic non-centrosymmetric  $P2_12_12_1$  space group with  $Z = 4$  [Figure S6(l)]. A short and highly directional C–H...F interaction ( $2.32$  Å,  $168^\circ$ ,  $-3.87$  kcal/mol), involving the highly acidic hydrogen H13 with F1, steers the packing of molecules along the crystallographic *a*-axis [Figure 12a, Table 2a]. In addition, weak C–H... $\pi$  (involving H4 with Cg2) interaction forms molecular chains along the crystallographic *b*-axis generating a sheet-like structure. The packing of

the molecules in **12** also displays the formation of the herringbone pattern, with the utilization of weak C–H...N (involving H8 with N1) and C–H... $\pi$  (involving H4 and H10) intermolecular interactions [Figure 12b, Table 2].

**13. N-(4-Fluorobenzylidene)aniline.** Compound **13** crystallizes in the triclinic centrosymmetric space group  $P\bar{1}$  with  $Z = 2$  [Figure S6m]. The packing of the molecules in the crystal involves the formation of molecular sheets down the *ac* plane with the utilization of bifurcated weak C–H...F intermolecular interactions, involving H11 and H9 with F1 ( $-1.27$  kcal/mol and  $-1.33$  kcal/mol respectively) [Figure 13a]. Further, these sheets are stabilized by dimeric C–H...N (involving H6 with N1,  $-1.29$  kcal/mol) and C–H... $\pi$  intermolecular interactions, involving acidic H3 and H5 with electron rich phenyl ring Cg2 and H8 with Cg1 [Figure 13b] (Table 2).

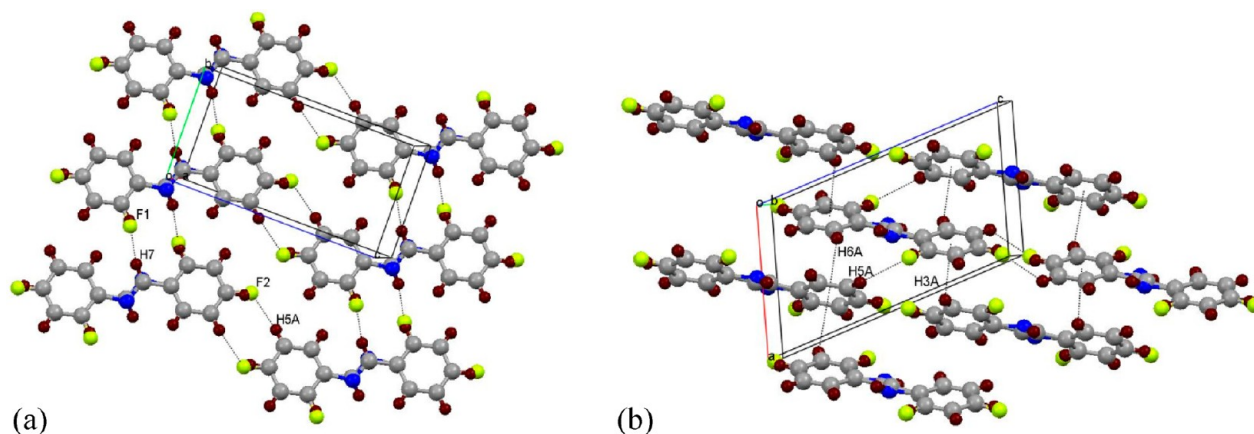


**Figure 7.** (a) Packing of 7 down the *bc* plane showing the formation of the molecular sheet *via* weak C–H...F intermolecular interactions. (b) The weak C–H... $\pi$  and C–H...F intermolecular interactions viewed down the *ac* plane in 7.

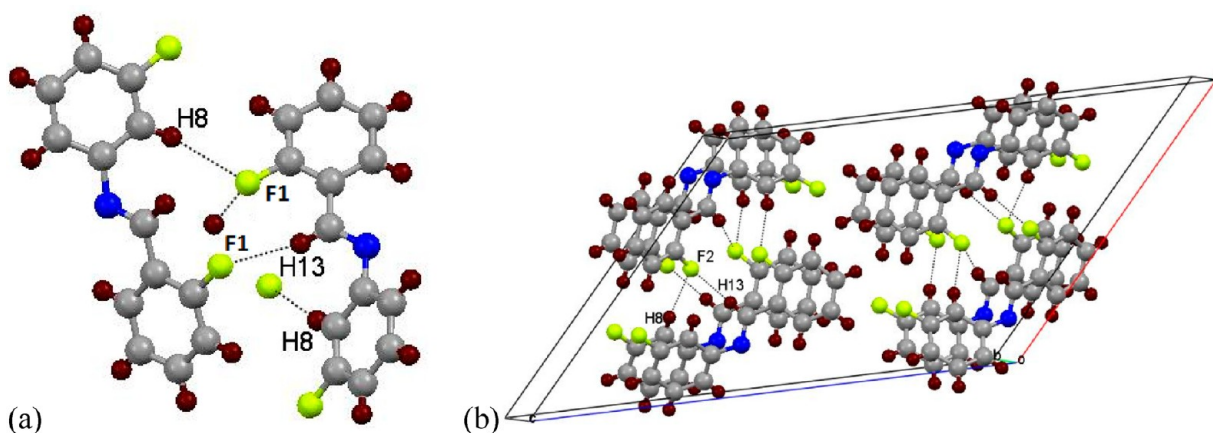


**Figure 8.** (a) Formation of molecular heterodimeric motif by weak C–H...F intermolecular interactions in 8. (b) Packing view down the *ac* plane shows extension of dimers in 8.

**14. *N*-(3-Fluorobenzylidene)aniline.** This compound was found to be a liquid at 25 °C. Attempts to grow a single crystal using *in situ* crystallization technique failed. The compound formed a glass on cooling and did not show any signature of crystallization on several cooling and heating cycles using the Oxford cryosystem. This was followed by repeated attempts to allow for sudden heating by OHCD and sudden cooling by switching off the CO<sub>2</sub> LASER. Hence, the structure for this compound could not be determined.

**15. *N*-(2-Fluorobenzylidene)aniline.** This compound was also found to be liquid at 25 °C. Several attempts to crystallize the compound by cooling it to 200–150 K failed. OHCD was also used to trigger crystallization by sudden thermal shock to the liquid at 200 K. But all our efforts failed to crystallize 15. Hence, the structure for this compound could not be determined.

## DISCUSSION

The detailed analysis of these 13 crystal structures in the series of fluorine substituted *N*-benzylideneanilines allows for a better understanding of the role of weak intermolecular interactions which stabilize the crystal packing in the absence of any strong hydrogen bonds. The crystal packing in these compounds are found to be mainly governed by the presence of short, highly directional (in some cases >165°) C–H...F and C–H... $\pi$  interactions [Table 2]. The interaction energies associated with

the weak C–H...F interactions for different supramolecular motifs have been evaluated. These are given in Table 2a, which have interaction energies ranging from 1 to 5 kcal/mol and are stabilizing in nature. It has also been established from electron density studies,<sup>34</sup> crystallographic database, and computational evidence<sup>35</sup> that C–H...F interactions have weak hydrogen bond character. It is also of significance to note that C–H...F hydrogen bonds with a H...F distance between 2.2 and 2.67 Å and the angle  $\angle$ C–H...F ranging between 130 and 168° have higher interaction energies (3 kcal/mol or more). Presumably these weak C–H...F hydrogen bonds thereby influence the preorganization of the molecules in the formation of molecular layers, and such layer of molecules are held with the adjacent layers by the involvement of weak C–H... $\pi$  interactions and additional independent C–H...F hydrogen bonds. C–H... $\pi$  interactions have recently received major recognition in all fields of chemistry and biology. It has been debated whether it has a hydrogen bond character or is essentially dispersive in nature. The latest developments in the supramolecular chemistry of C–H... $\pi$  are summarized in authoritative articles by Nishio and co-workers.<sup>36</sup> The results of PIXEL calculations are shown in the Table S2. It is observed that the lattice energies of these compounds are between 22 and 27 kcal/mol, although these compounds have a range of different crystal structures, which display a variety of supramolecular synthons.

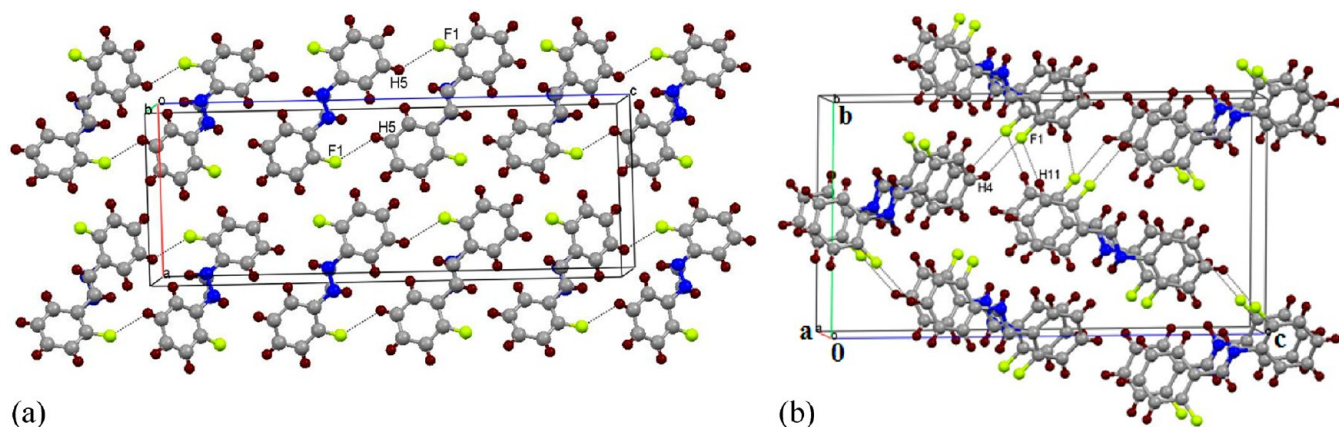


**Figure 9.** (a) The packing of the polymorph I of **9** viewed down the  $ac$  plane displays the generation of molecular sheet of dimers formed *via* C–H...F intermolecular interactions. (b) The packing of polymorph II of **9** viewed down the  $bc$  plane, showing the formation of a molecular sheet *via* C–H...F intermolecular interactions.

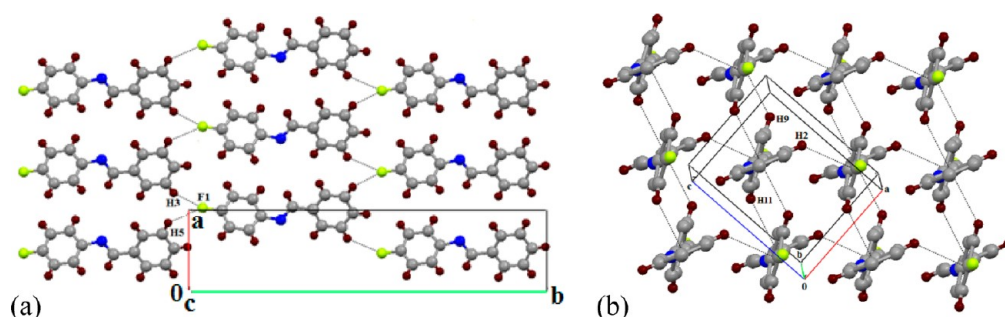


**Figure 10.** (a) View down the  $ab$  plane, depicting the formation of a molecular sheet *via* weak C–H...F intermolecular interactions in **10**. (b) The packing of molecules down the  $ac$  plane, depicting C–H... $\pi$  intermolecular interactions in **10**.

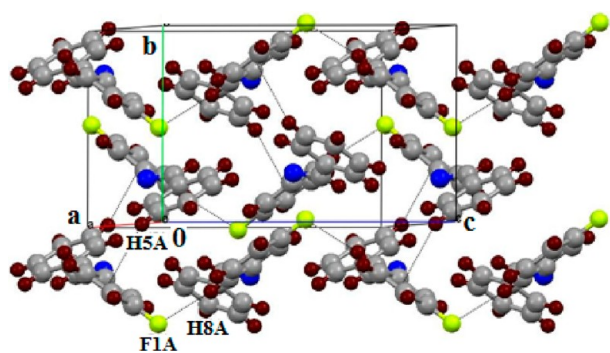


**Figure 11.** Packing of molecules *via* weak C–H...F and C–H... $\pi$  intermolecular interactions in **11**.

It is of active interest to compare the similarities and differences, which occur in the molecular conformation and the crystal packing on substitution of the fluorine atom (responsible for altered packing motifs) on the molecular skeleton containing the *N*-benzylideneaniline moiety. The parent compound, *N*-benzylideneaniline, was found to exist in the monoclinic  $P2_1/c$  space group with  $Z = 4$  [ $a = 12.1211(9)$  Å,  $b = 7.7182(5)$  Å,  $c = 11.8429(9)$  Å,  $\beta = 118.341(1)^\circ$ ].<sup>18d</sup> The conformational features associated with these molecules in the solid state present some interesting features when compared with the torsion values obtained from theoretical calculations. For the torsion angle C6–C1–C13–N1 the theoretical values are close to planarity. The theoretical value for the torsion C8–C7–N1–C13 with respect to the aniline ring remains essentially constant between 31–43°,

to minimize the repulsion of the phenyl ring with the nitrogen lone pair of electrons. The corresponding experimental torsion angle lies in the range of 35–50° [except for compounds **2**, **4**, **5**, **7**, and **9** (polymorph II)] and are almost similar to that of *N*-benzylideneaniline. Compounds **5** and **7** are nearly planar (high energy conformation), and the stabilization essentially comes from the positional disorder associated with the C=N bond in addition to the crystallographic disorder about the inversion center associated with half of the molecule in the asymmetric unit. For the torsion C1–C13–N1–C7, both the experimental and theoretical values are close to planarity (Table 3).

The molecular packing in the crystal of *N*-benzylideneaniline<sup>18d</sup> consists of the arrangement of the molecules with their long axis parallel to the crystallographic  $a$ -axis [Figure 14]. The substitution of the fluorine atom at *ortho* position in case of **12** completely alters the crystal structure (orthorhombic  $P2_12_12_1$ ) in comparison to the unsubstituted one. It is of interest to note that the substitution of the fluorine atom at the *meta* position in *N*-benzylideneaniline (compound **11**) did not alter the cell parameters and close packing of molecules, hence displaying isostructurality<sup>37</sup> with the parent compound. The incorporation of a fluorine atom at the *para* position on either phenyl ring (compounds **10** and **13**) has resulted in the formation of a different crystal structure compared to the unsubstituted analogue. Although the former (**10**) crystallizes in the monoclinic  $P2_1/n$  space group, the lattice parameters and crystal packing were found to be different than those of the parent compound, while the latter (**13**) crystallizes in triclinic  $P\bar{1}$ . However compounds **10** and **13** have similar packing, the relationship between the lattice parameters being  $a = a'$ ;  $b = 2c'$ ;  $c = b'$  wherein  $a$ ,  $b$ ,  $c$  and  $a'$ ,  $b'$ ,  $c'$  are

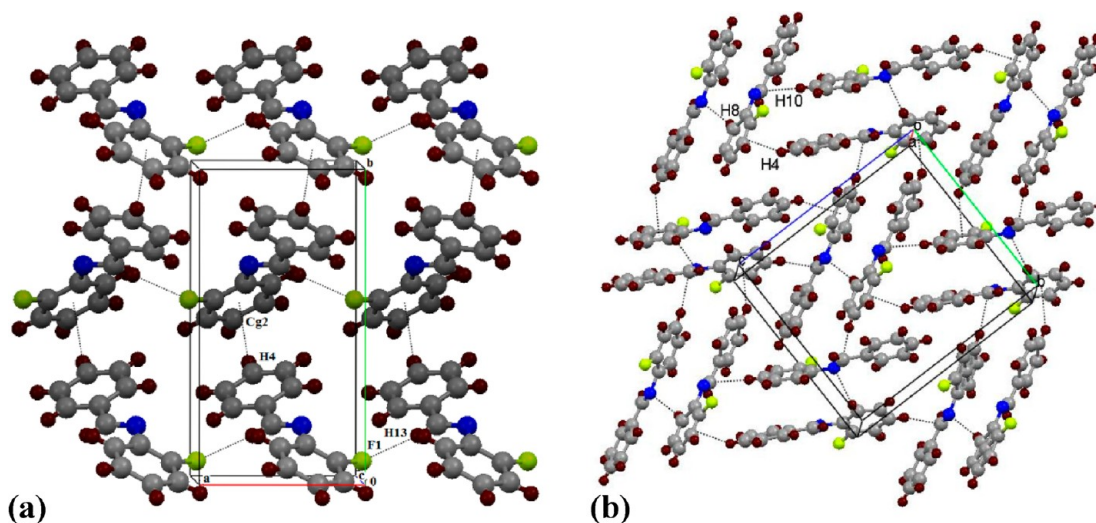


**Figure 12.** (a) Packing view down the *ab* crystallographic plane via weak C–H...F and C–H... $\pi$  intermolecular interactions in **12**. (b) The weak C–H...N and C–H... $\pi$  interactions dictate the formation of a herringbone sheet down the *bc* plane in **12**.

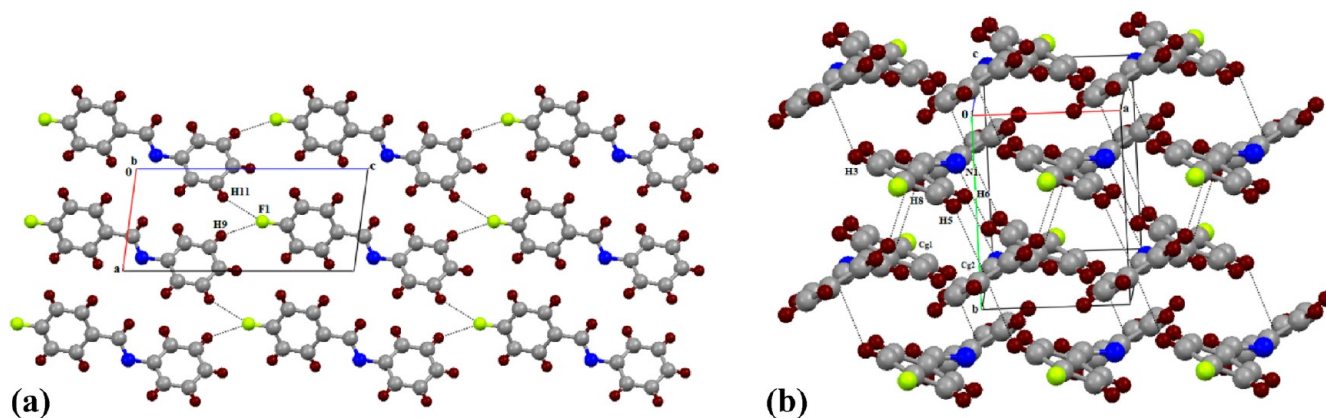


**Figure 13.** (a) Molecular sheet down the *ac* plane via bifurcated weak C–H...F intermolecular interactions in **13**. (b) Packing of molecules in **13** via weak C–H... $\pi$  and C–H...N intermolecular interactions.

the lattice parameters of **10** and **13** respectively. Another notable feature is the fact that compounds **1** (difluorinated) and **13** (monofluorinated) crystallize in an identical space group (triclinic  $P\bar{1}$ ), **1** and **13** being essentially isostructural in the solid state [Figures 1b and 13b]. Compounds **1** and **13** are also isostructural with 4-fluoro-*N*-(4-fluorophenyl)benzamide.<sup>8b</sup> It is also important to note that the crystal packing of difluorinated *N*-benzylideneanilines, namely, **2**, **5**, **7**, **8**, and **9** (polymorph I), were found to be different from *N*-benzylideneanilines. Among these as well, the crystal packing is found to be different from each other as the supramolecular synthons observed in these structures are different, except in the case of compounds **5** and **7**, which exhibit isostructurality [Figures 5 and 7b]. It is also of importance that **10** has double the unit cell volume of **5** or **7** and the crystal packing is also similar with the latter, the lattice parameters being related by  $a = c'$ ;  $b = a'$ ;  $c = b'/2$  where  $a$ ,  $b$ ,  $c$  and  $a'$ ,  $b'$ ,  $c'$  are the lattice parameters of **5/7** and **10** respectively. Furthermore, it is to be noted that compounds **6** and **12** crystallized in the orthorhombic noncentrosymmetric  $P2_12_12_1$  space group and also exhibit isostructural behavior [Figures 6b and 12b]. Compound **9** which consists of fluorine atoms in the *ortho* position in both the phenyl rings crystallizes in two polymorphic forms, the monoclinic form being centrosymmetric

and the orthorhombic form being non-centrosymmetric. Both the forms exhibit positional disorder with respect to the position of the C=N bond and are distinguished in terms of the nature of weak C–H...F hydrogen bonds in their crystal lattices.

The Cambridge Structural Database<sup>38</sup> search<sup>39</sup> has been performed for *N*-benzylideneaniline derivatives to compare the molecular conformation and crystal packing of related compounds with the present series of compounds. Table 4 lists all the related structures containing one functional group present on either or both the phenyl rings. Crystal structures which contain any strong hydrogen bond donor (e.g., hydroxyl and amino groups) or acceptor (amino nitrogen and oxygen) groups have not been considered [ETEYUX, LIXJIL, TIQRU, ZEXPEX, ZEXPEX01, ZEXPEX02].

The bromo (BRZBRA),<sup>40a</sup> chloro (CBZCAN01),<sup>17a,b</sup> and cyano (AMEREQ)<sup>40b</sup> analogues of **1** have been found to display different crystal structures as compared to that of **1**. The triclinic form of the compound CBZCAN exists in a planar conformation, whereas the orthorhombic form CBZCAN01 exists in a nonplanar conformation, which is disordered with respect to the 2-fold crystallographic axis. CBZCAN and compound **1** have a different molecular conformation, the former being planar and the latter nonplanar. The resulting crystal packing is different as

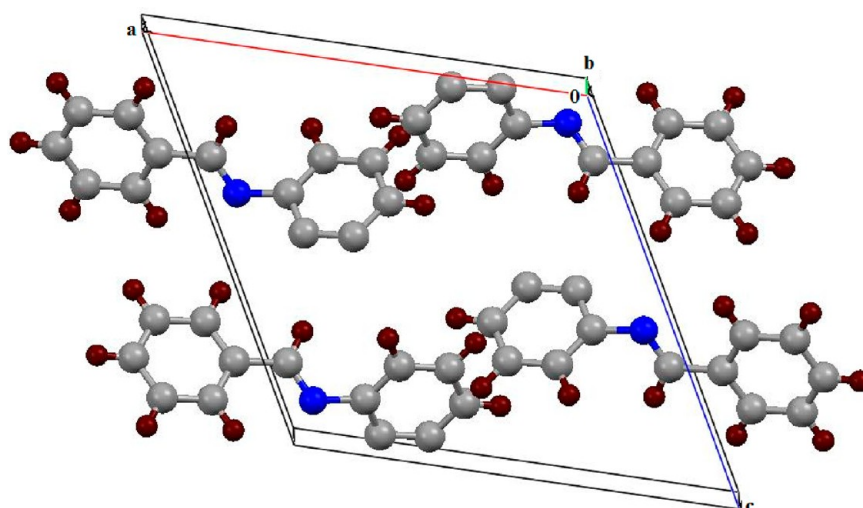


Figure 14. Packing view of *N*-benzylideneanilines (NBA) down the *ac*-plane.

Table 4. List of Unit Cell Parameters and Torsion Angles of *N*-Benzylideneaniline and Its Derivatives Reported in the CSD

compound name CCDC REFCODE	space group; cell parameter	torsion angles		
		C8–C7–N1–C13	C6–C1–C13–N1	C1–C13–N1–C7
<i>N</i> -benzylideneaniline BENZON10	( <i>P2</i> <sub>1</sub> / <i>c</i> ); 12.157, 7.921, 11.944, 118.38	56.83	9.92	179.51
<i>p</i> -cyano- <i>N</i> -( <i>p</i> -cyanobenzylidene)aniline AMEREQ	( <i>P2</i> <sub>1</sub> / <i>c</i> ); 4.727(0), 10.443(2), 11.943(2), 98.70(3)	1.14	1.14	180.00
<i>N</i> -( <i>p</i> -Bromobenzylidene)- <i>p</i> -bromoaniline <sup>a</sup> BRZBRA	( <i>P2</i> <sub>1</sub> / <i>a</i> ); 24.912(13), 5.877(1), 4.046(1), 92.42(3)	2.20, 2.20 <sup>a</sup>	2.20, 2.20 <sup>a</sup>	180.00, 180.00 <sup>a</sup>
<i>N</i> -( <i>p</i> -chlorobenzylidene)- <i>p</i> -chloroaniline <sup>a</sup> CBZCAN	( <i>P1</i> ); 5.986(2), 3.933(1), 12.342(2), 87.38(3), 78.40(3), 89.53(3)	0.12, 0.12 <sup>a</sup>	0.12, 0.12 <sup>a</sup>	180.00, 180.00 <sup>a</sup>
<i>N</i> -( <i>p</i> -chlorobenzylidene)- <i>p</i> -chloroaniline <sup>a</sup> CBZCAN01	( <i>Pccn</i> ); 24.503(5), 6.334(1), 7.326(1)	26.67, 26.67 <sup>a</sup>	26.67, 26.67 <sup>a</sup>	179.38, 179.38 <sup>a</sup>
<i>N</i> -( <i>p</i> -chlorobenzylidene)- <i>m</i> -chloroaniline RONKEK	( <i>P2</i> <sub>1</sub> ); 10.742(4), 4.820(2), 11.634(5), 109.25(2)	0.48	2.65	179.08
<i>N</i> -( <i>p</i> -bromobenzylidene)- <i>m</i> -bromoaniline RONKIO	( <i>P2</i> <sub>1</sub> ); 11.113(2), 4.796(2), 11.886(2), 109.55(3)	0.98	3.78	176.68
<i>N</i> -( <i>p</i> -bromobenzylidene)- <i>m</i> -chloroaniline RONKOU	( <i>P2</i> <sub>1</sub> ); 11.030(2), 4.750(2), 11.670(2), 109.66(3)	1.62	1.76	178.01
<i>N</i> -( <i>p</i> -chlorobenzylidene)- <i>m</i> -bromoaniline RONKUA	( <i>P2</i> <sub>1</sub> ); 10.840(2), 4.740(2), 11.630(2), 108.57(3)	0.15	3.15	179.16
<i>N</i> -( <i>m</i> -chlorobenzylidene)- <i>p</i> -bromoaniline RONLAH	( <i>P2</i> <sub>1</sub> / <i>c</i> ); 8.609(6), 5.989(4), 23.437(14), 93.66(2)	44.04	9.61	175.49
<i>N</i> -( <i>m</i> -bromobenzylidene)- <i>p</i> -bromoaniline RONLEL	( <i>P2</i> <sub>1</sub> / <i>c</i> ); 8.630(2), 6.050(2), 23.226(5), 92.34(3)	41.88	9.99	175.46
<i>N</i> -( <i>m</i> -chlorobenzylidene)- <i>m</i> -chloroaniline <sup>a</sup> WEMHUR	( <i>P2</i> <sub>1</sub> / <i>n</i> ); 25.231(6), 3.943(1), 12.002(3), 102.64(2)	37.73, 23.09 <sup>a</sup>	27.14, 12.85 <sup>a</sup>	164.51, 166.57 <sup>a</sup>
<i>N</i> -( <i>m</i> -chlorobenzylidene)- <i>m</i> -bromoaniline <sup>a</sup> WEMJAZ	( <i>P2</i> <sub>1</sub> 2 <sub>1</sub> 2 <sub>1</sub> ); 9.615(2), 31.336(7), 3.967(2)	17.02, 29.27 <sup>a</sup>	30.15, 18.25 <sup>a</sup>	179.56, 178.75 <sup>a</sup>
<i>N</i> -( <i>m</i> -bromobenzylidene)- <i>m</i> -bromoaniline WEMJED	( <i>P2</i> <sub>1</sub> 2 <sub>1</sub> 2 <sub>1</sub> ); 9.646(3), 31.552(7), 4.007(2)	39.13	11.62	179.57
<i>N</i> -( <i>m</i> -bromobenzylidene)- <i>m</i> -chloroaniline WEMJIH	( <i>P2</i> <sub>1</sub> 2 <sub>1</sub> 2 <sub>1</sub> ); 7.842(3), 13.644(7), 11.096(7)	40.41	3.79	176.39
( <i>E</i> )-4-bromo- <i>N</i> -(2-chlorobenzylidene)aniline EVONEJ	( <i>P2</i> <sub>1</sub> / <i>n</i> ); 15.243(13), 4.020(4), 20.142(18), 103.25(0)	43.46	5.99	176.77

<sup>a</sup>Another torsion angle due to the presence of disorder around the C=N bond.

they utilize different types of interactions. The former (chlorine substitution at *para* position on both side) utilize Cl⋯Cl interactions with no C–H⋯Cl contacts in crystal packing while the latter have C–H⋯F hydrogen bonds only and no F⋯F contact.

Furthermore, substitution of other halogens, namely, bromo and chloro [*para* to benzaldehyde side and *meta* to aniline side], does not alter the crystal structure (monoclinic, non-centrosymmetric

*P2*<sub>1</sub>) in most of the cases [RONKEK<sup>40c</sup> (Cl, *p*, *m*); RONKIO<sup>40c</sup> (Br, *p*, *m*); RONKOU<sup>40c</sup> (Br, *p*; Cl, *m*); RONKUA<sup>40c</sup> (Cl, *p*; Br, *m*)], the lattice parameters depicting isostructurality. In contrast, the related fluoro compound **2** crystallizes in the monoclinic centrosymmetric *P2*<sub>1</sub>/*c* space group. In cases of related halogen substitution, *meta* to benzaldehyde side and *para* to aniline side, two compounds RONLAH<sup>40c</sup> (Cl, *m*; Br, *p*), RONLEL<sup>40c</sup> (Br, *m*, *p*),

crystallizes in the corresponding centrosymmetric monoclinic,  $P2_1/c$  exhibiting isostructural behavior with  $Z' = 1$  (Table 4). The related fluoro compound **4** crystallizes in the triclinic  $P\bar{1}$  with  $Z' = 2$  molecules in the asymmetric unit.

Further, the comparison of crystal structures of other halogen substituted *N*-benzylideneanilines [*meta* to both the benzaldehyde and aniline moieties] resulted in the following CSD REFCODES. WEMHUR<sup>40d</sup> (Cl, *m*, *m*) (crystallizes in monoclinic  $P2_1/n$ ) was found to be different than that of the related halogenated analogue WEMJAZ<sup>40d</sup> (Cl, *m*; Br, *m*), WEMJED<sup>30d</sup> (Br, *m*, *m*), WEMJIH<sup>40d</sup> (Br, *m*; Cl, *m*), which crystallized in the orthorhombic non-centrosymmetric  $P2_12_12_1$  space group (Table 4). Among these only WEMJAZ and WEMJED are found to be isostructural. The only reported analogue of compound **7** in the CSD is 4-bromo-*N*-(2-chlorobenzylidene)aniline (EVONEJ),<sup>40c</sup> and the crystal packing was found to be completely different from the fluorinated compound (Table 4).

It is evident from the above-mentioned features of differently substituted *N*-benzylideneanilines that the incorporation of fluorine atoms in both the rings at different positions have resulted in a variety of molecular structures, wherein positional and crystallographic disorder play a significant role thereby exhibiting conformational differences in the solid state. On careful study of Table 2a, it may be noted that the C–H...F hydrogen bonds having interaction energy >4 kcal/mol show significant directionality ( $\angle\text{C–H...F} > 160^\circ$ ) with one exception. These crystal structures display a variety of well-defined supramolecular motifs, which steer the modified packing of molecules utilizing those interactions involving “organic fluorine” in the absence of strong hydrogen bond donors and acceptors. These observations further provide evidence of the directionality and the stabilizing influence of the C–F group in altering the crystal packing through the presence of weak but cooperative C–H...F hydrogen bonds. The packing is further supported by weak C–H... $\pi$  interactions involving an aromatic ring and also the isolated double bond.

## CONCLUSION

In the current manuscript, we have shown the importance of the C–F group in a series of mono- and difluorinated benzylideneanilines by single crystal X-ray diffraction studies performed at low temperature. The *N*-benzylideneaniline molecular skeleton allows for an evaluation of the changes which get manifested when a fluorine atom is substituted on the phenyl ring and its position is allowed to vary over the phenyl ring. This electronic feature results in conformational changes in different mono- and difluorinated benzylideneanilines, in addition to the presence of positional disorder in this class of molecules. It is evident from the detailed analysis of the structures of these molecules and related compounds in the CSD containing different halogens and other groups that there is a delicate interplay of steric and electronic factors which govern the final molecular conformation and subsequent crystal packing in these compounds. This also has implications in the serendipitous phenomenon of polymorphism in the solid state. It is also of importance to note that the aromatic C–F group(s) in the absence of strong hydrogen bonding functional groups are capable of significantly influencing the crystal structures of small organic molecules. The interaction energy calculations show that these hydrogen bonds have energies ranging from 1 to 5 kcal/mol. Several supramolecular motifs (namely dimers and chains) based on C–H...F hydrogen bonds have been observed in these structures. Our efforts to investigate the capability of “organic fluorine”

in the presence of other halogens on the *N*-benzylideneaniline scaffold are currently in progress. The role of organic fluorine in altering crystal structures in the presence of other halogens and related functional groups will be the key focus aimed toward an improved understanding of interhalogen interactions in the solid state.

## ASSOCIATED CONTENT

### Supporting Information

Crystallographic information file; melting point of solid compounds determined from DSC data; results of CLP calculations; dihedral angles; FTIR spectra, <sup>1</sup>H NMR, DSC traces of solids; powder X-ray data; profile fitting refinement with the cell parameters for both the forms; ORTEP of all compounds. This material is available free of charge via the Internet at <http://pubs.acs.org>.

## AUTHOR INFORMATION

### Corresponding Author

\*(A.R.C.) E-mail: [angshurc@iisermohali.ac.in](mailto:angshurc@iisermohali.ac.in), phone: 0091-172-2240266; (D.C.) E-mail: [dchopra@iiserb.ac.in](mailto:dchopra@iiserb.ac.in), phone: 0091-755-4092321.

### Author Contributions

#These authors have contributed equally.

### Notes

The authors declare no competing financial interest.

## ACKNOWLEDGMENTS

G.K. thanks CSIR, India, and P.P. thanks UGC, India, for a research fellowship. A.R.C. and G.K. thank Dr. Kabirul Islam for useful discussions. We thank IISER Mohali for Single Crystal X-ray and NMR facilities; IISER Bhopal for FTIR and DSC measurements, and IISc Bangalore for PXRD measurements. Both IISER Mohali and IISER Bhopal are acknowledged for research and all other infrastructural facilities. D.C. thanks DST-Fast track scheme for research funding.

## REFERENCES

- (1) Philip, D.; Stoddart, J. F. *Angew. Chem., Int. Ed.* **1996**, *35*, 1154–1196.
- (2) Desiraju, G. R.; Steiner, T. *The Weak Hydrogen Bond in Structural Chemistry and Biology*; Oxford University Press: Oxford, 1999.
- (3) (a) Pimentel, G. C.; McLella, A. L. *Hydrogen Bond*; Freeman: San Francisco, 1960. (b) Pauling, L. *The Nature of Chemical Bond*; Cornell University Press; Ithaca, New York, 1960. (c) Jeffrey, G. A.; Sanger, W. *Hydrogen Bonding in Biological Structures*; Springer, Berlin, 1991.
- (d) Desiraju, G. R. *Angew. Chem., Int. Ed.* **2011**, *50*, 52–59.
- (4) Jeffrey, G. A. *Crystallogr. Rev.* **2003**, *9*, 135–176.
- (5) (a) Reichenbacher, K.; Suss, H. I.; Hulliger, J. *Chem. Soc. Rev.* **2005**, *34*, 22–30. (b) O'Hagan, D. *Chem. Soc. Rev.* **2008**, *37*, 308–319. (c) Howard, J. A. K.; Hoy, V. J.; O'Hagan, D.; Smith, G. T. *Tetrahedron.* **2006**, *52*, 12613–12622. (d) Dunitz, J. D.; Taylor, R. *Chem. Eur. J.* **1997**, *3*, 89–98. (e) Dunitz, J. D. *ChemBioChem* **2004**, *5*, 614–621.
- (6) (a) Berger, R.; Resnati, G.; Metrangolo, P.; Weber, E.; Hulliger, J. *Chem. Soc. Rev.* **2011**, *40*, 3496–3508 and references therein. (b) Chopra, D.; Guru Row, T. N. *CrystEngComm* **2011**, *13*, 2175–2186 and references therein. (c) Chopra, D. *Cryst. Growth Des.* **2012**, *12*, 541–546.
- (7) (a) Choudhury, A. R.; Urs, U. K.; Smith, P. S.; Goddard, R.; Howard, J. A. K.; Guru Row, T. N. *J. Mol. Struct.* **2002**, *641*, 225–232. (b) Choudhury, A. R.; Guru Row, T. N. *Cryst. Growth Des.* **2004**, *4*, 47–52. (c) Chopra, D.; Nagarajan, K.; Guru Row, T. N. *J. Mol. Struct.* **2008**, *888*, 70–83.

- (8) (a) Chopra, D.; Guru Row, T. N. *Cryst. Growth Des.* **2005**, *5*, 1679–1681. (b) Chopra, D.; Guru Row, T. N. *CrystEngComm* **2008**, *10*, 54–67. (c) Chopra, D.; Guru Row, T. N. *Cryst. Growth Des.* **2008**, *8*, 848–853. (d) Nayak, S. K.; Reddy, M. K.; Guru Row, T. N.; Chopra, D. *Cryst. Growth Des.* **2011**, *11*, 1578–1596. (e) Panini, P.; Chopra, D. *CrystEngComm* **2012**, *14*, 1972–1989.
- (9) (a) Nuss, G. W., Jr.; Santora, N. J.; Douglas, G. H. United States Patent, 1980, 4187317. (b) Nuss, G. W., Jr.; Santora, N. J.; Douglas, G. H. United States Patent, 1980, 4198349. (c) Cassidy, J. M.; Kiser, C. E.; Sabhapondit, A. United States Patent, 2011, 0155959A1.
- (10) (a) Burgi, H. B.; Dunitz, J. D.; Züst, C. *Acta Crystallogr.* **1968**, *B24*, 463–464. (b) Burgi, H. B.; Dunitz, J. D. *Chem. Commun.* **1969**, 472–473. (c) Robertson, J. M.; Woodward, I. *Proc. R. Soc.* **1937**, *A* (162), 568–583. (d) de Lange, J. J.; Robertson, J. M.; Woodward, I. *Proc. R. Soc.* **1939**, *A* (171), 398–410. (e) Brown, C. J. *Acta Crystallogr.* **1966**, *21*, 146–152.
- (11) Burgi, H. B.; Dunitz, J. D. *Helv. Chim. Acta* **1970**, *53*, 1747–1764.
- (12) Burgi, H. B.; Dunitz, J. D. *Helv. Chim. Acta* **1971**, *54*, 1255–1260.
- (13) (a) Bernstein, J.; Bar, I.; Christensen, A. *Acta Crystallogr.* **1976**, *B32*, 1609–1611. (b) Bar, I.; Bernstein, J. *Acta Crystallogr.* **1978**, *B33*, 1738–1744. (c) Bar, I.; Bernstein, J. *Acta Crystallogr.* **1982**, *B38*, 121–125.
- (14) Bernstein, J.; Engel, Y. M.; Hagler, A. T. *J. Chem. Phys.* **1981**, *75*, 2346–2353.
- (15) Bernstein, J.; Bar, I. *J. Phys. Chem.* **1982**, *86*, 3223–3231.
- (16) Beasley, A. G.; Welberry, T. R.; Goossens, D. J.; Heerdegen, A. P. *Acta Crystallogr.* **2008**, *B64*, 633–643.
- (17) (a) Bernstein, J.; Schmidt, G. M. J. *J. Chem. Soc. Perkin Trans II.* **1972**, 951–955. (b) Bernstein, J.; Izak, I. *J. Chem. Soc. Perkin Trans II.* **1976**, 429–424. (c) Hagler, A. T.; Bernstein, J. *J. Am. Chem. Soc.* **1978**, *100*, 673–681. (d) Hagler, A. T.; Bernstein, J. *J. Am. Chem. Soc.* **1978**, *100*, 6349–6354.
- (18) (a) Harada, J.; Ogawa, K.; Tomoda, S. *Acta Crystallogr.* **1997**, *B53*, 662–672. (b) Harada, J.; Ogawa, K. *J. Am. Chem. Soc.* **2001**, *123*, 10884–10888. (c) Ojala, W. H.; Lystad, K. M.; Deal, T. L.; Engebretson, J. E.; Spude, J. M.; Balidemaj, B.; Ojala, C. R. *Cryst. Growth Des.* **2009**, *9*, 964–970. (d) Harada, J.; Harakawa, M.; Ogawa, K. *Acta Crystallogr.* **2004**, *B60*, 578–588. (e) Harada, J.; Harakawa, M.; Ogawa, K. *Acta Crystallogr.* **2004**, *B60*, 589–597.
- (19) Nayak, S. K.; Reddy, M. K.; Chopra, D.; Guru Row, T. N. *CrystEngComm* **2012**, *14*, 200–210.
- (20) (a) Thalladi, V. R.; Weiss, H. –C.; Bläser, D.; Boese, R.; Nangia, A.; Desiraju, G. R. *J. Am. Chem. Soc.* **1998**, *120*, 8702–8710. (b) Choudhury, A. R.; Winterton, N.; Steiner, A.; Cooper, A. I.; Johnson, K. A. *J. Am. Chem. Soc.* **2005**, *127*, 16792–16793. (c) Choudhury, A. R.; Islam, K.; Kirchner, M. T.; Mehta, G.; Guru Row, T. N. *J. Am. Chem. Soc.* **2004**, *126*, 12274–12275.
- (21) Macrae, C. F.; Bruno, I. J.; Chisholm, J. A.; Edgington, P. R.; McCabe, P.; Pidcock, E.; Rodriguez-Monge, L.; Taylor, R.; Streek, J.; Wood, P. A. *J. Appl. Crystallogr.* **2008**, *41*, 466–470.
- (22) Petricek, V.; Dusek, M.; Palatinus, L. *Jana2000*, 08/11/2007 ed.; Institute of Physics: Praha, Czech Republic, 2007.
- (23) APEX2, SADABS and SAINT; Bruker AXS Inc.: Madison, Wisconsin, USA, 2008.
- (24) Dolomanov, O. V.; Bourhis, L. J.; Gildea, R. J.; Howard, J. A. K.; Puschmann, H. *J. Appl. Crystallogr.* **2009**, *42*, 339–341.
- (25) Farrugia, L. J. WinGx. *J. Appl. Crystallogr.* **1999**, *32*, 837–838.
- (26) Sheldrick, G. M. *Acta Crystallogr.* **2008**, *A64*, 112–122.
- (27) Nardelli, M. *J. Appl. Crystallogr.* **1995**, *28*, 659.
- (28) Spek, A. L. *Acta Crystallogr.* **2009**, *D65*, 148–155.
- (29) <http://www.ohcd-system.com/infos/infos.htm>.
- (30) Bondi, A. *J. Phys. Chem.* **1964**, *68*, 441–451.
- (31) Schmidt, M. W.; Baldrige, K. K.; Boatz, J. A.; Elbert, S. T.; Gordon, M. S.; Jensen, J. H.; Koseki, S.; Matsunaga, N.; Nguyen, K. A.; Su, S. J.; Windus, T. L.; Dupuis, M.; Montgomery, A., Jr. *PC GAMESS*, version 6.4; *J. Comput. Chem.* **1993**, *14*, 1347–1363.
- (32) Gavezzotti, A. *New J. Chem.* **2011**, *35*, 1360–1368.
- (33) Allouche, A. R. *J. Comput. Chem.* **2011**, *32*, 174–182.
- (34) Chopra, D.; Cameron, T. S.; Ferrara, J. D.; Guru Row, T. N. *J. Phys. Chem. A.* **2006**, *110*, 10465–10477.
- (35) (a) D’Oria, E.; Novoa, J. J. *CrystEngComm* **2008**, *10*, 423–436. (b) Schneider, H. J. *Chem. Sci.* **2012**, *3*, 1381–1394.
- (36) (a) Nishio, M.; Umezawa, Y.; Honda, K.; Tsuboyama, S.; Suezawa, H. *CrystEngComm* **2009**, *11*, 1757–1788. (b) Takahashi, O.; Kohno, Y.; Nishio, M. *Chem. Rev.* **2010**, *110*, 6049–6076. (c) Nishio, M. *Phys. Chem. Chem. Phys.* **2011**, *13*, 13873–13900.
- (37) Kálmán, A.; Párnányi, L.; Argay, G. *Acta Crystallogr.* **1993**, *B49*, 1039–1049.
- (38) Allen, F. H. *Acta Crystallogr.* **2002**, *B58*, 380–388.
- (39) CSD version 5.33 (November 2011): The following constraints were applied: No REFCODE restrictions applied, 3D coordinates determined, R factor  $\leq 0.1$ , No errors, Not polymeric, No ions, Only Organics.
- (40) (a) Bernstein, J.; Izak, I. *J. Chem. Crystallogr.* **1975**, *5*, 257–266. (b) Ojala, C. R.; Ojala, W. H.; Britton, D. *J. Chem. Crystallogr.* **2011**, *41*, 464–469. (c) Navon, O.; Bernstein, J. *Struct. Chem.* **1997**, *8*, 3–11. (d) Zamir, S.; Bernstein, J. *Acta Chim. Hung.* **1993**, *130*, 301–325. (e) Wang, C. *Acta Crystallogr.* **2011**, *E67*, o2204.